Published for SISSA by Springer

Received: October 11, 2023
Accepted: April 17, 2024
Published: May 15, 2024

Mechanical structure of the nucleon and the baryon octet: twist-2 case

Ho-Yeon Won[a,b] **Hyun-Chul Kim**[a,c] **and June-Young Kim**[d]

[a]*Department of Physics, Inha University, Incheon 22212, Republic of Korea*
[b]*CPHT, CNRS, École polytechnique, Institut Polytechnique de Paris, 91120 Palaiseau, France*
[c]*School of Physics, Korea Institute for Advanced Study (KIAS), Seoul 02455, Republic of Korea*
[d]*Theory Center, Jefferson Lab, Newport News, VA 23606, U.S.A.*

E-mail: hoyeon.won@polytechnique.edu, hchkim@inha.ac.kr, jykim@jlab.org

Abstract: We investigate the gravitational form factors (GFFs) of the nucleon and the baryon octet, decomposed into their flavor components, utilizing a pion mean-field approach grounded in the large N_c limit of Quantum Chromodynamics (QCD). Our focus is on the contributions from the twist-2 operators to the flavor-triplet and octet GFFs, and we decompose the mass, angular momentum, and D-term form factors of the nucleon into their respective flavors. The strange quark contributions are found to be relatively mild for the mass and angular momentum form factors, while providing significant corrections to the D-term form factor. In the course of examining the flavor decomposition of the GFFs, we uncover that the effects of twist-4 operators play a crucial role. While the gluonic contributions are suppressed by the packing fraction of the instanton vacuum in the twist-2 case, contributions from twist-4 operators are of order unity, necessitating its explicit consideration.

Keywords: Properties of Hadrons, Effective Field Theories of QCD, Parton Distributions

ArXiv ePrint: 2310.04670

https://doi.org/10.1007/JHEP05(2024)173

Contents

1 Introduction

Strangeness in the nucleon has been one of the most crucial issues in comprehending the underlying structure of the nucleon. Since the European Muon Collaboration (EMC) announced the puzzling measurement that the quark intrinsic spin provides only a small portion of the proton's spin [1, 2], there has been a great amount of experimental and theoretical works (see a review [3] and references therein). It is now known that the quark intrinsic spin carries approximately 35 % of the proton's spin [3]. The rest will come from the orbital angular momenta of the quarks and the total angular momentum of the gluons inside a proton. The EMC results triggered an idea to measure the strange contributions to the electromagnetic form factors (EMFFs) of the proton [4], and the strange vector form factors were extracted from parity-violating electron-proton scattering [5–10] and theoretically (refer to a recent review and references therein for further details [11]). Although the strange magnetic moment

JHEP05(2024)173

is relatively small, it remains significant. For instance, the strange magnetic form factor at $Q^2 \simeq 0.1, \mathrm{GeV}^2$ was determined to be 0.30 ± 0.17 [11]. Additionally, the πN sigma term, which contributes to the nucleon mass, incorporates contributions from the strange quark. Specifically, approximately 20 % of the πN sigma term is attributed to the strange quark [12]. Furthermore, investigations have been carried out to explore the strange-quark contribution to the nucleon tensor charge [13, 14].

The role of strange quarks can also extend to the gravitational form factors (GFFs) [15, 16] of the nucleon, which provide crucial insights into the properties of the nucleon, including its mass, spin, mechanical pressure, and shear force [17, 18]. Although the concept of the GFFs was introduced about sixty years ago [15, 16], experimental access to them had been limited, so that they were regarded as a purely academic interest. However, the emergence of generalized parton distributions (GPDs) [19–22] has paved the way for extracting experimental information on the GFFs. It is possible to measure the obesrvables related to the GFFs because the EMFFs and GFFs can be understood as the first and second Mellin moments of vector GPDs, respectively [17].

To perform the flavor decomposition of the GFFs, we need to consider the flavor triplet and octet energy-momentum tensor (EMT) currents, which are not conserved [23]. Consequently, they can not be derived from the Nöther theorem. In QCD, they can still be constructed by using the conserved singlet EMT current as a guide [24], which consist of the twist-2 and higher-twist terms. Moreover, the gluonic degrees of freedom come into crucial play. While the gluonic contribution is suppressed by the packing fraction of the instanton vacuum in the case of the twist-2 operators, we find that the contributions from twist-4 operators are of order unity [25, 26]. It implies that, without the gluonic contributions considered, it is not possible to perform a complete analysis of the flavor decomposition of the GFFs. In ths current work, thus, we focus on the twist-2 contributions to the flavor decomposition of the GFFs and distributions, and discuss why the twist-4 operators must be taken into account. Since it is technically far involved in deriving the effective twist-4 operators corresponding to the QCD operators, we leave it as a future work and concentrate on the role of the twist-2 operators in the flavor decomposition of the GFFs and corresponding distributions, and discuss why the twist-2 operators only are not sufficient for interpreting the flavor-decomposed distributions of the nucleon as mechanical properties.

Bearing in mind the problems posed above, we use the chiral quark-soliton model (χQSM), which was developed based on large N_c QCD [27, 28]. In the large N_c limit of QCD, a classical baryon can be regarded as N_c valence quarks bound by a mesonic mean field that arises as a classical solution of the saddle point equation in a self-consistent manner, while the quantum fluctuations are suppressed and of order $1/N_c$. Since the classical baryon has no good quantum numbers, the zero-mode quantization is required to restore the translational and rotational symmetries. These rotational and translational zero modes naturally give rise to the standard SU($2N_f$) spin-flavor symmetry in the large N_c limit of QCD [29–31].

The χQSM as a chiral theory of the nucleon was originally derived from the QCD instanton vacuum [32, 33]. The low-energy effective partition function of QCD was be obtained, which realizes the spontaneous breakdown of chiral symmetry, and satisfies the relevant low-energy theorems. It is important to note that the gluon degrees of freedom have

JHEP05(2024)173

been integrated out through the instanton vacuum, and their effects are incorporated into the momentum-dependent dynamical quark mass M. In the χQSM, we switch off the momentum dependence of M and introduce a regularization to tame the divergent quark loops. The χQSM has been successful in describing the breakdown of the Gottfried sum rule [34, 35], the light-flavor asymmetry [36–38] of polarized parton distribution functions (PDFs), and the transversity distributions [39–41]. It has also provided a satisfactory explanation for the contributions of strange quarks to axial charges [42, 43] and vector charges [44, 45]. For a comprehensive overview, refer to the reviews [46, 47].

Finally, we want to address the issue of three-dimensional (3D) mechanical interpretation of the GFFs. The 3D EMT distributions have been proposed as the Fourier transform of the GFFs [18, 48]. However, the 3D interpretation of the EMT distributions has faced significant criticism [49–53]. Due to the inability to precisely localize the nucleon wave packet below the Compton wavelength, there are ambiguous relativistic corrections to the 3D distributions (see ref. [54]). To deal with this ambiguity, a two-dimensional (2D) light-front (LF) distribution has been used [50–52]. In the current work, however, we adhere to the 3D interpretation of the EMT distributions.

As discussed in a number of works considering the large N_c limit [55, 56], the center of motion of the nucleon exhibits a non-relativistic behavior (while the nucleon itself possesses fully relativistic internal dynamics). Therefore, information about the 3D distributions is conveyed into the 2D space on the light cone with no change. The frame dependence of these distributions has been explored in ref. [55] in the context of the large N_c limit. In addition, it was very recently found that the 3D components of the EMT can be matched with the 2D light-front components [56]. While considering the admixture of the 3D components in this matching, the Melosh rotation (IMF Wigner rotation [57]) effects under the Lorentz boost are suppressed in the large N_c limit. Consequently, the light-front helicity state becomes equivalent to the canonical spin state at rest.

The structure of the current paper is as follows: in section 2, we recapitulate a definition of the Belinfante-Rosenfeld EMT current in QCD and express the matrix element of the EMT current, which is parametrized in terms of the GFFs. We decompose the EMT current in terms of the twist, and corresponding matrix elements. We also discuss the 3D mechanical interpretations associated with these GFFs. In section 3, we offer a brief explanation of the χQSM and illustrate the spin-flavor properties of the GFFs in flavor SU(3) symmetry. In section 4, we discuss the numerical results on the 3D EMT distributions. Furthermore, we present the flavor-decomposed GFFs for the baryon octet using the spin-flavor symmetry, and discuss the incompleteness of the current scheme. Finally, in section 5 we provide a summary of our work and draw conclusions based on our findings.

2 QCD energy-momentum tensor

According to Ji's decomposition [20] (see also refs. [58, 59]), the quark (q) and gluon parts (g) of the Belinfante-Rosenfeld-type QCD EMT currents are expressed as

$$T_q^{\mu\nu} = \frac{i}{4}\bar{\psi}_q\left(\gamma^{\{\mu}\overleftrightarrow{\mathcal{D}}^{\nu\}}\right)\psi_q, \quad T_g^{\mu\nu} = -F^{\mu\rho,a}F^{\nu,a}_{\ \ \rho} + \frac{1}{4}g^{\mu\nu}F^{\lambda\rho,a}F^{a}_{\lambda\rho}, \tag{2.1}$$

JHEP05(2024)173

where $\overleftrightarrow{\mathcal{D}}^{\mu} = \overleftrightarrow{\partial}^{\mu} - 2igA^{\mu}$ is the covariant derivative with $\overleftrightarrow{\partial}^{\mu} = \overrightarrow{\partial}^{\mu} - \overleftarrow{\partial}^{\mu}$, and $a^{\{\mu}b^{\nu\}} = a^{\mu}b^{\nu} + a^{\nu}b^{\mu}$. $F^{b,\mu\nu}$ is the gluon field strength, where the superscript b indicates the color index. This EMT current consists of the quark (q) and gluon (g) parts, and is a conserved quantity:

$$T^{\mu\nu} = \sum_{q} T_q^{\mu\nu} + T_g^{\mu\nu}, \quad \partial_\mu T^{\mu\nu} = 0. \tag{2.2}$$

However, if we consider the separate quark and gluon EMT currents, they are not conserved anymore.

In addition, we will discuss the twist-projected EMT current and emphasize the importance of the higher-twist part in the mechanical interpretation of the EMT distributions. The symmetric part of the EMT current can be divided into the twist-2 (spin-2) and twist-4 (spin-0) parts, which are associated with the leading twist vector GPDs and twist-4 GPDs, respectively. These twist-projected EMT currents are given by

$$T_a^{\mu\nu} = \bar{T}_a^{\mu\nu} + \hat{T}_a^{\mu\nu}, \tag{2.3}$$

where the twist-2 ($\bar{T}_a^{\mu\nu}$) and twist-4 ($\hat{T}_a^{\mu\nu}$) parts are defined by

$$\bar{T}_a^{\mu\nu} = T_a^{\mu\nu} - \frac{1}{4} g^{\mu\nu} T_{a,\alpha}^{\alpha}, \quad \hat{T}_a^{\mu\nu} = \frac{1}{4} g^{\mu\nu} T_{a,\alpha}^{\alpha}, \tag{2.4}$$

with $a = q, g$. Note that the twist-3 part is related to the asymmetric EMT current, which is not discussed in this work.

2.1 Matrix element of the energy-momentum tensor current

The matrix element of the EMT current can be described by four independent Lorentz-invariant functions, namely A^a, J^a, D^a, and $\bar{c}^a$, which are obtained by considering all possible Lorentz structures and sorting them out by using the discrete symmetries (hermiticity, time reversal, and parity). This parameterization has been studied extensively in previous works [15, 16, 60, 61] (For further information on the generalization of this parametrization, interested readers may refer to refs. [62, 63]). The baryon matrix element of the EMT current is expressed as

$$\begin{aligned}\langle B(p', J_3')|T_{\mu\nu}^a(0)|B(p, J_3)\rangle = \bar{u}(p', J_3')\Bigg[& A_B^a(t)\frac{P_\mu P_\nu}{M_B} + J_B^a(t)\frac{iP_{\{\mu}\sigma_{\nu\}\rho}\Delta^\rho}{2M_B} \\ & + D_B^a(t)\frac{\Delta_\mu\Delta_\nu - g_{\mu\nu}\Delta^2}{4M_B} + \bar{c}_B^a(t) M_B g_{\mu\nu}\Bigg] u(p, J_3),\end{aligned} \tag{2.5}$$

where A^a, J^a, D^a, and $\bar{c}^a$ are called the mass, angular momentum, D-term, and cosmological constant term form factors of a baryon B, respectively. When considering the separate operators for quarks and gluons, they are no more conserved. This leads to the appearance of an additional form factor, denoted by $\bar{c}$ in the flavor decomposition. As a consequence, the form factors of individual quarks and gluons exhibit both scale and scheme dependence. For brevity, the dependence of the renormalization scale of the individual quark and gluon GFFs is not indicated in this work. The normalization of the one-particle state for the baryon is expressed as $\langle B'(p', J_3')|B(p, J_3)\rangle = 2p^0(2\pi)^3\delta_{J_3'J_3}\delta^{(3)}(\boldsymbol{p'} - \boldsymbol{p})$, where J_3 and J_3' denote the

JHEP05(2024)173

spin polarizations of the initial and final states, respectively. The M_B represents the mass of a baryon, while p and p' refer to the initial and final momenta, respectively. We define $P = (p' + p)/2$ and $\Delta = p' - p$, where $\Delta^2 = t$, to represent the average momentum and the momentum transfer between the initial and fianl states, respectively. We express the GFFs generically as F_B^χ, where the flavor indices run over $\chi = 0, 3, 8$. They can be decomposed in terms of the quark components

$$F_B^{\chi=0} = F_B^u + F_B^d + F_B^s, \quad F_B^{\chi=3} = F_B^u - F_B^d, \quad F_B^{\chi=8} = \frac{1}{\sqrt{3}}\left(F_B^u + F_B^d - 2F_B^s\right). \tag{2.6}$$

Thus, the GFFs of a baryon are given by the sum of all quark and gluon contributions

$$\sum_{a=q,g} F_B^a(t) = F_B(t), \quad \bar{c}_B(t) = 0. \tag{2.7}$$

Note that the current conservation imposes the constraint that $\bar{c}(t)$ is zero. In this respect, the $\bar{c}$ form factor should carefully be considered when we do the flavor decomposition, or look into the quark and gluon subsystems.

In fact, extracting the $\bar{c}$ form factor is challenging in most dynamical models and lattice QCD due to the higher-twist (twist-4) corrections. To isolate this twist-4 term in a most systematic way, we can decompose the symmetrized EMT current in terms of the twist-2 and twist-4 components, as presented in eq. (2.3). With these twist-projected EMT currents employed, we define their nucleon matrix elements as follows:

$$\begin{aligned}
&\langle B(p', J_3')|\bar{T}^a_{\mu\nu}(0)|B(p, J_3)\rangle \\
&= \bar{u}(p', J_3')\Bigg[A_B^a(t)\frac{P_\mu P_\nu}{M_B} + J_B^a(t)\frac{iP_{\{\mu}\sigma_{\nu\}\rho}\Delta^\rho}{2M_B} + D_B^a(t)\frac{\Delta_\mu\Delta_\nu - tg^{\mu\nu}}{4M_B} \\
&\quad - g_{\mu\nu}\left\{\frac{t}{8M_B}J_B^a(t) - \frac{3t}{16M_B}D_B^a(t) + \frac{M_B}{4}\left(1 - \frac{t}{4M_B^2}\right)A_B^a(t)\right\}\Bigg]u(p, J_3),
\end{aligned} \tag{2.8}$$

and

$$\begin{aligned}
&\langle B(p', J_3')|\hat{T}^a_{\mu\nu}(0)|B(p, J_3)\rangle \\
&= \bar{u}(p', J_3')\Bigg[g_{\mu\nu}\Bigg\{M_B\bar{c}_B^a(t) + \frac{t}{8M_B}J_B^a(t) \\
&\qquad - \frac{3t}{16M_B}D_B^a(t) + \frac{M_B}{4}\left(1 - \frac{t}{4M_B^2}\right)A_B^a(t)\Bigg\}\Bigg]u(p, J_3).
\end{aligned} \tag{2.9}$$

Furthermore, since higher-twist operators are strongly constrained by the QCD equation of motion, it is very useful to partition the QCD operators in terms of the twist so that these constraints can explicitly be confirmed in the nucleon matrix elements, for example,

$$\langle B(p', J_3')|\hat{T}^q_{\mu\nu}(0)|B(p, J_3)\rangle = 0, \quad \text{in the chiral limit.} \tag{2.10}$$

Note that one can obviously see that the sum of the above twist-2 and twist-4 parts is equal to the parametrization in eq. (2.5):

$$\langle B(p', J_3')|T^q_{\mu\nu}(0)|B(p, J_3)\rangle = \langle B(p', J_3')|\bar{T}^q_{\mu\nu}(0)|B(p, J_3)\rangle + \langle B(p', J_3')|\hat{T}^q_{\mu\nu}(0)|B(p, J_3)\rangle. \tag{2.11}$$

JHEP05(2024)173

2.2 Three-dimensional distribution

To gain insight into the mechanical interpretation of the GFFs in the position space, one can perform the Fourier transformation of these form factors. This approach was first explored in ref. [18] and was inspired by the concept used in EMFFs and their charge and magnetization distributions. However, the interpretation of EMFFs and GFFs in terms of the 3D distributions has been criticized [49–54, 64] due to the inherent limitations imposed by the Compton wavelength, which prevents the precise localization of the nucleon wave packet. Consequently, this limitation introduces ambiguous relativistic corrections to the 3D distribution.

One perspective suggests that if the nucleon is treated as a non-relativistic object (where the initial and final wave packets become equivalent and well-localized), the form factor [65] can be understood as a 3D distribution. However, if one insists on using the strict definition of the distribution, we can consider the following approach: if we consider the infinite momentum frame or the light-front formalism, then ambiguous relativistic corrections are kinematically suppressed, effectively rendering the system non-relativistic. However, we have to pay the cost of losing longitudinal information, reducing the distribution to a 2D one. Another way is to take a conceptual detour in the treatment of 3D distributions. From a Wigner phase space perspective [57, 66–68], the 3D distribution can be regarded as quasi-probabilistic, reflecting the internal dynamics of the hadron, with all ambiguous relativistic corrections encapsulated in the Wigner distributions. Furthermore, recent developments have introduced the definition of 3D spatial distributions in the zero average momentum frame [69–71].

Since the 2D IMF provides clear and unambiguous definitions of EMT distributions, we can choose to work within that frame. However, in the context of the large N_c limit, it is both natural and sufficient to focus on the 3D distribution. While the internal dynamics of the nucleon is fully described within a relativistic framework (including all the relativistic motions of the quarks), the center of motion of the nucleon is treated in a non-relativistic manner due to the $1/N_c$ suppression. This means that translational corrections, such as $\boldsymbol{P}^2/2M_N \sim \mathcal{O}(N_c^{-1})$, to the nucleon energy are parametrically suppressed, and the same suppression applies to the nucleon GFFs. Consequently, the soliton nature of the nucleon is inherently static and collectively non-relativistic. A related discussion of this topic can be found in ref. [55]. Moreover, the large N_c approximation causes the equivalence between the light-front helicity state and the canonical spin state at rest. This allows one to perform *matching* [56] between the 3D components of the EMT and the 2D LF ones.

In the Breit frame, the quark and gluon components of the GFFs are determined by taking the Fourier transforms of the matrix element of the EMT current between the initial and final states of the baryon. This definition is found in ref. [18]:

$$\mathcal{O}^{a,B}_{\mu\nu}(\boldsymbol{r}, J_3', J_3) = \int \frac{d^3\Delta}{(2\pi)^3 2P^0} e^{-i\boldsymbol{\Delta}\cdot\boldsymbol{r}} \langle B(p', J_3')|\mathcal{O}^a_{\mu\nu}(0)|B(p, J_3)\rangle, \tag{2.12}$$

with $\mathcal{O} = \{T, \bar{T}, \hat{T}\}$.

In the following subsections, we will mainly discuss the role of the twist-2 and twist-4 GFFs in the 3D mechanical interpretation, focusing on the importance of the twist-4 pieces in the EMT distributions. For example, when performing flavor decomposition and partitioning the

JHEP05(2024)173

quark gluon subsystems, it is inappropriate to discuss the mechanical interpretations in terms of the twist-2 part only, such as local stability conditions, mechanical raidus, and mass radius.

2.3 Mass distribution

The temporal components $\mathcal{O} = \{T, \bar{T}, \hat{T}\}$ of the EMT currents are related to the quark and gluon contributions to the mass distributions $f = \{\varepsilon, \bar{\varepsilon}, \hat{\varepsilon}\}$ inside a baryon

$$f_B^a(r)\delta_{J_3'J_3} := \mathcal{O}_{00}^{a,B}(\boldsymbol{r}, J_3', J_3) = M_B \int \frac{d^3\Delta}{(2\pi)^3} e^{-i\boldsymbol{\Delta}\cdot\boldsymbol{r}} F_B^a(t)\delta_{J_3'J_3}, \tag{2.13}$$

where the 3D mass (monopole) form factors $F = \{\mathcal{E}, \bar{\mathcal{E}}, \hat{\mathcal{E}}\}$ are given by

$$\mathcal{E}_B^a(t) = \left[A_B^a(t) + \bar{c}_B^a(t) - \frac{t}{4M_B^2}\left(A_B^a(t) - 2J_B^a(t) + D_B^a(t)\right)\right], \tag{2.14a}$$

$$\bar{\mathcal{E}}_B^a(t) = \frac{3}{4}\left[A_B^a(t) - \frac{t}{4M_B^2}\left(A_B^a(t) - 2J_B^a(t) + \frac{1}{3}D_B^a(t)\right)\right], \tag{2.14b}$$

$$\hat{\mathcal{E}}_B^a(t) = \frac{1}{4}\left[A_B^a(t) + 4\bar{c}_B^a(t) - \frac{t}{4M_B^2}\left(A_B^a(t) - 2J_B^a(t) + 3D_B^a(t)\right)\right]. \tag{2.14c}$$

Note that we have obvious relations

$$\mathcal{E}_B^a(t) = \bar{\mathcal{E}}_B^a(t) + \hat{\mathcal{E}}_B^a(t), \quad \varepsilon_B^a(r) = \bar{\varepsilon}_B^a(r) + \hat{\varepsilon}_B^a(r). \tag{2.15}$$

In the forward limit, they are connected to the A and $\bar{c}$ form factors:

$$\mathcal{E}_B^a(0) = A_B^a(0), \quad \bar{\mathcal{E}}_B^a(0) = \frac{3}{4}A_B^a(0), \quad \hat{\mathcal{E}}_B^a(0) = \frac{1}{4}A_B^a(0) + \bar{c}_B^a(0). \tag{2.16}$$

By integrating the spatial components of the EMT currents ($\mathcal{O}_{00}^{a,B}$) over space, the mass of a spin-1/2 baryon at rest can be calculated as

$$\int d^3r \varepsilon_B^a(r) = M_B\mathcal{E}_B(0) = M_B[A_B^a(0) + \bar{c}_B^a(0)], \tag{2.17a}$$

$$\int d^3r \bar{\varepsilon}_B^a(r) = M_B\bar{\mathcal{E}}_B(0) = M_B\frac{3}{4}[A_B^a(0)], \tag{2.17b}$$

$$\int d^3r \hat{\varepsilon}_B^a(r) = M_B\hat{\mathcal{E}}_B(0) = M_B\frac{1}{4}[A_B^a(0) + 4\bar{c}_B^a(0)], \tag{2.17c}$$

with

$$\int d^3r f_B(r) = \int d^3r \sum_{a=q,g} f_B^a(r) = M_B\left\{1, \frac{3}{4}, \frac{1}{4}\right\}, \tag{2.18}$$

and the normalized mass form factor $A_B(0) = 1$, where the contribution of $\bar{c}_B$ to ε_B is zero due to the conservation of the EMT current. However, the equations (2.17a) and (2.17c) imply that when we split the energy distributions into the quark and gluon parts, they start to be subject to the $\bar{c}_B^a$ form factor. In other words, the twist-2 distribution (2.17b) is only independent of the $\bar{c}$ form factor.

JHEP05(2024)173

The size of the mass distribution can be expressed in terms of the mass radius. Intuitively, we impose the following condition

$$\varepsilon_B^a > 0, \tag{2.19}$$

which can be confirmed numerically within the current work. This positivity of the energy distribution allows us to define the mass radius for separate quark and gluon contributions. It is given by either the integral of the mass distribution or the derivative of the form factors $6\left[A_B(t) - \frac{t}{4M_B^2} D_B(t)\right]$ with respect to the momentum squared,

$$\sum_{a=q,g} \left\langle r^2_{\text{mass}} \right\rangle_B^a = \frac{\sum_{a=q,g} \int d^3r\, r^2 \varepsilon_B^a(r)}{\sum_{a=q,g} \int d^3r\, \varepsilon_B^a(r)} = 6\frac{d}{dt}\left[A_B(t) - \frac{t}{4M_B^2} D_B(t)\right]_{t=0}. \tag{2.20}$$

Once we do the flavor decomposition of the mass radius, we then have the contribution from $\bar{c}_B^a$, which must not be neglected.

2.4 Angular momentum distribution

The mixed components of the EMT current ($T_{0i}^{a,B}$) are associated with the total angular momentum (AM) distributions [sum of spin and orbital angular momentum (OAM)] by the Belinfante and Rosenfeld construction. The definition of the total AM distributions inside a baryon is given by the AM operator in QCD as follows:

$$\begin{aligned} J_i^{a,B}(\boldsymbol{r}, J_3', J_3) :=& \epsilon_{ijk} r_j T_{0k}^{a,B}(\boldsymbol{r}, J_3', J_3) \\ =& 2\left(\hat{S}_j\right)_{J_3' J_3} \int \frac{d^3\Delta}{(2\pi)^3} e^{-i\boldsymbol{\Delta}\cdot\boldsymbol{r}} \left[\left(J_B^a(t) + \frac{2}{3} t \frac{dJ_B^a(t)}{dt}\right)\delta_{ij} \right. \\ & \left. + \left(\Delta_i\Delta_j - \frac{1}{3}\boldsymbol{\Delta}^2\delta_{ij}\right)\frac{dJ_B^a(t)}{dt}\right]. \end{aligned} \tag{2.21}$$

In the following discussion, we will separate it into its monopole and quadrupole parts. Note, however, that the quadrupole distribution is related to the monopole distribution [18, 59, 72]. For the purpose of this discussion, we refer to the monopole distribution [18] as the AM distribution, which can be expressed as follows

$$\rho_{J,B}^a(r) := \int \frac{d^3\Delta}{(2\pi)^3} e^{-i\boldsymbol{\Delta}\cdot\boldsymbol{r}} \left[\left(J_B^a(t) + \frac{2}{3} t \frac{dJ_B^a(t)}{dt}\right)\right]. \tag{2.22}$$

Integrating both $J_i^{a,B}(\boldsymbol{r}, J_3', J_3)$ and $\rho_{J,B}^a(r)$ over 3D space yields the spin of the baryon as follows

$$\int d^3r \sum_{a=q,g} J_i^{a,B}(\boldsymbol{r}, J_3', J_3) = 2\left(\hat{S}_i\right)_{J_3' J_3} J_B(0) = \left(\hat{S}_i\right)_{J_3' J_3}, \tag{2.23}$$

with $\rho_{J,B}(r) = \sum_{a=q,g} \rho_{J,B}^a(r)$. The AM form factor $J_B(0)$ is normalized to 1/2 to ensure that the integral of the AM distribution $J_i^{a,B}(\boldsymbol{r}, J_3', J_3)$ over space is equivalent to the spin operator of a baryon. Note that the quadrupole component has no effect on the spin normalization.

The decomposition of the angular momentum into the OAM and the quark spin requires the twist-3 component of the EMT (the antisymmetric part of the EMT current), which is

JHEP05(2024)173

not discussed in this paper. For more information on the separation of the OAM and the quark spin using the QCD equation of motion, see refs. [58, 59, 73, 74]. In addition, the $J(t)$ form factor (angular momentum distributions) comes from the off-diagonal components of the EMT, so it is not affected by the twist-4 contribution. Therefore, the definition of the 3D distributions remains intact, unaffected by the twist classification. In other words, the flavor decomposition can be performed unambiguously without higher-twist contribution.

2.5 Mechanical properties

The spatial components of the EMT, denoted by $T^{a,B}_{ij}$, give information about the mechanical properties of a baryon. They include the pressure and shear-force distributions, i.e., $f = \{p, \bar{p}, \hat{p}\}$ and s, respectively, inside a baryon. By decomposing $\mathcal{O} = \{T, \bar{T}, \hat{T}\}$ into irreducible tensors, the pressure and shear-force distributions are related to rank 0 and rank 2 tensors, respectively:

$$\mathcal{O}^{a,B}_{ij}(\boldsymbol{r}, J'_3, J_3) = f^a_B(r)\delta^{ij}\delta_{J'_3 J_3} + s^a_B(r)\left(\frac{r^i r^j}{r^2} - \frac{1}{3}\delta^{ij}\right)\delta_{J'_3 J_3}. \tag{2.24}$$

The pressure and shear-force distributions are defined as

$$\begin{aligned} f^a_B(r) &= M_B \int \frac{d^3\Delta}{(2\pi)^3} e^{-i\boldsymbol{\Delta}\cdot\boldsymbol{r}} F^a_B(t), \\ s^a_B(r) &= -\frac{1}{4M_B} r \frac{d}{dr}\frac{1}{r}\frac{d}{dr}\int \frac{d^3\Delta}{(2\pi)^3} e^{-i\boldsymbol{\Delta}\cdot\boldsymbol{r}} D^a_B(t), \end{aligned} \tag{2.25}$$

where the pressure form factors $F = \{\mathcal{P}, \bar{\mathcal{P}}, \hat{\mathcal{P}}\}$ are listed as

$$\begin{aligned} \mathcal{P}^a_B(t) &= \left[-\bar{c}^a_B(t) + \frac{t}{6M_B^2} D^a_B(t)\right], \\ \bar{\mathcal{P}}^a_B(t) &= \frac{1}{4}\left[A^a_B(t) - \frac{t}{4M_B^2}\left(A^a_B(t) - 2J^a_B(t) + \frac{1}{3}D^a_B(t)\right)\right], \\ \hat{\mathcal{P}}^a_B(t) &= -\frac{1}{4}\left[A^a_B(t) + 4\bar{c}^a_B(t) - \frac{t}{4M_B^2}\left(A^a_B(t) - 2J^a_B(t) + 3D^a_B(t)\right)\right]. \end{aligned} \tag{2.26}$$

Note that we have obvious relations

$$\mathcal{P}^a_B(t) = \bar{\mathcal{P}}^a_B(t) + \hat{\mathcal{P}}^a_B(t), \quad p^a_B(r) = \bar{p}^a_B(r) + \hat{p}^a_B(r). \tag{2.27}$$

At the zero momentum transfer $t \to 0$, they are reduced to

$$\mathcal{P}^a_B(0) = -\bar{c}^a_B(0), \quad \bar{\mathcal{P}}^a_B = \frac{1}{4}A^a_B(0), \quad \hat{\mathcal{P}}^a_B = -\frac{1}{4}A^a_B(0) - \bar{c}^a_B(0). \tag{2.28}$$

The pressure and shear-force distributions can be expressed as the Fourier transforms of the $F = \{\mathcal{P}, \bar{\mathcal{P}}, \hat{\mathcal{P}}\}$ and D-term form factors

$$\begin{aligned} F^a_B(t) &= \frac{1}{M_B}\int d^3r\, j_0(r\sqrt{-t}) f^a_B(r), \\ D^a_B(t) &= 4M_B \int d^3r\, \frac{j_2(r\sqrt{-t})}{t} s^a_B(r). \end{aligned} \tag{2.29}$$

JHEP05(2024)173

Interestingly, the twist-projected 3D multipole energy and pressure form factors are related to each other:

$$\bar{\mathcal{P}}^a_B(t) = \frac{1}{3}\bar{\mathcal{E}}^a_B(t), \quad \hat{\mathcal{P}}^a_B(t) = -\hat{\mathcal{E}}^a_B(t). \tag{2.30}$$

This means that the twist-projected energy and pressure distributions are also related to each other as follows:

$$\bar{\varepsilon}^a_B(r) = 3\bar{p}^a_B(r), \quad \hat{\varepsilon}^a_B(r) = -\hat{p}^a_B(r). \tag{2.31}$$

While the distributions of the gluon and quark shear forces, which arise from the off-diagonal component of the EMT, do not depend on $\bar{c}^a(t)$ form factor, the knowledge of $\bar{c}^a(t)$ form factor is required to determine the pressure distributions. Therefore, the unambiguous definition of the 3D pressure distribution is not possible without the twist-4 form factors considered.

Now we are in a position to discuss the stability conditions The distributions of the stress tensors p_B and s_B, which represent the sum of each parton contribution ($p_B := \sum_{a=q,g} p^a_B$, $s_B := \sum_{a=q,g} s^a_B$), are strongly constrainted by the conservation of the EMT current. This constraint is expressed by the equilibrium equation:

$$\frac{\partial}{\partial r}\left(\frac{2}{3}s_B(r) + p_B(r)\right) + \frac{2s_B(r)}{r} = 0, \tag{2.32}$$

which connects the pressure distribution to the shear-force one. Analyzing the individual contributions of the partons to these distributions, we discover an intriguing equilibrium equation that relates the quark and gluon subsystems, which is expressed by the continuity equation:

$$\sum_{a=q,g} \partial^i T^{a,B}_{ij} = \sum_{a=q,g} \frac{r_j}{r}\left[\frac{2}{3}\frac{\partial s^a_B(r)}{\partial r} + \frac{2s^a_B(r)}{r} + \frac{\partial p^a_B(r)}{\partial r}\right] = \sum_{q=u,d,s} \tilde{f}^q_{B,j} + \tilde{f}^g_{B,j} = 0, \tag{2.33}$$

where the internal force between the quarks and gluon inside the baryon is represented as

$$\tilde{f}^a_{B,j} = -M_B \frac{\partial}{\partial r^j}\int \frac{d^3\Delta}{(2\pi)^3} e^{-i\boldsymbol{\Delta}\cdot\boldsymbol{r}} \bar{c}^a_B(t). \tag{2.34}$$

As a consequence of eq. (2.33) for a mechanically stable baryon, the sum of the internal forces $\tilde{f}^a_{B,j}$ between the partons must cancel out each other. Additionally, integrating eq. (2.25) over space leads to a critical stability criterion known as the von Laue stability condition:

$$\int_0^\infty dr\ r^2 p_B(r) = 0. \tag{2.35}$$

This condition implies that the pressure distribution must have at least one nodal point where it becomes null. Furthermore, another stability criterion, proposed in several works [75–77], is worth mentioning. Perevalova et al. [75] introduced a local stability criterion that states a specific combination of the pressure and shear-force distributions must be positive (outward) at any given distance r:

$$\frac{2}{3}s_B(r) + p_B(r) > 0. \tag{2.36}$$

JHEP05(2024)173

This function can be interpreted as the normal force field, while the tangential force can be expressed as $-\frac{1}{3}s_B(r) + p_B(r)$. Furthermore, the positivity of the shear-force distribution over r in eq. (2.32), i.e., $s_B(r) > 0$, implies that $\frac{2}{3}s_B(r) + p_B(r) > 0$ is a monotonically decreasing function. To quantify the mechanical size of a baryon system, the mechanical radius is defined as:

$$\sum_{a=q,g} \langle r^2_{\rm mech}\rangle^a_B = \frac{\sum_{a=q,g}\int d^3r\; r^2\left(\frac{2}{3}s^a_B(r) + p^a_B(r)\right)}{\sum_{a=q,g}\int d^3r\;\left(\frac{2}{3}s^a_B(r) + p^a_B(r)\right)} = \frac{6D_B(0)}{\int^0_{-\infty} D_B(t)dt}. \tag{2.37}$$

Regardless of knowing the $\bar{c}$ form factor, the stability condition is satisfied, since it is a quantity that adds up all partonic contributions, i.e. $\sum_{a=q,g}\bar{c}^a_B = 0$. Thus, the higher-twist form factor plays no role in the stability condition. However, when the quark and gluon subsystems are decomposed, the higher-twist form factor comes into essential play.

3 Chiral quark-soliton model

In this section, we briefly review the χQSM.

3.1 Classical nucleon

The χQSM is based primarily on two fundamental principles: chiral symmetry breaking and the large N_c limit of QCD. This model is constructed, based on the effective partition function of QCD, which is applicable in the low-energy regime. In Euclidean space, the partition function is expressed as

$$Z_{\rm eff} = \int \mathcal{D}\psi^\dagger \mathcal{D}\psi \mathcal{D}U \exp(-S_{\rm eff}), \quad S_{\rm eff} = \int d^4x\, \psi^\dagger \left(i\partial\!\!\!/ + iMU^{\gamma_5} + i\hat{m}\right)\psi, \tag{3.1}$$

where M denotes the dynamical quark mass. It is orginally given as a momentum-dependent one $M(k)$, where k stands for the quark momentum or quark virtuality. For simplicity, we switch off the momentum dependence of $M(k)$, and consider it as a free parameter. We fix its value by reproducing various nucleon form factors and the mass differences between the nucleon and the Δ baryon. The most favorable value of M is found to be 420 MeV, since various observables computed with that value were well reproduced [46]. $\hat{m}$ represents the diagonal matrix of the current quark masses in the SU(3) flavor space. We assume isospin symmetry, setting $\bar{m} = m_u = m_d$. While the strange current quark mass is typically treated perturbatively, its contributions to the GFFs are found to be small. Thus, we impose the flavor SU(3) symmetry, fixing $m_s = \bar{m}$.

Since we use the constant M, we have to tame the divergences arising from the quark-loop integrals. To deal with them, we introduce the proper-time regularization. We fix the cutoff mass Λ by fitting the pion decay constant $f_\pi = 93$ MeV, and determine the current quark mass $\bar{m}$ by reproducing the pion mass $m_\pi = 139$ MeV (see ref. [78] for more details).

The chiral field U^{γ_5} is represented by the U field:

$$U^{\gamma_5} = \frac{1+\gamma_5}{2}U + \frac{1-\gamma_5}{2}U^\dagger, \tag{3.2}$$

JHEP05(2024)173

with $U = \exp(i\pi^a\lambda^a)$. The π^a denote the pseudo-Nambu-Goldstone (pNG) fields, and λ^a designate the Gell-Mann matrices. In the pion mean-field approach, we consider the hedgehog symmetry, which is a minimal symmetry that align the spatial vector with the isospin vector in the mean field:

$$U^{\gamma_5}_{\mathrm{SU}(2)} = \exp[i\gamma_5 \hat{\boldsymbol{n}} \cdot \boldsymbol{\tau} P(r)], \tag{3.3}$$

where $\pi^a(\boldsymbol{r}) = \hat{n}^a P(r)$ with $\hat{n}^a = r^a/|\boldsymbol{r}|$ for $a = 1, 2, 3$, and $\pi^a(\boldsymbol{r}) = 0$ for $a = 4, \ldots 8$. This symmetry ensures the invariance of the pion mean field under $\mathrm{SU}(2)_{\mathrm{flavor}} \otimes \mathrm{SU}(2)_{\mathrm{spin}}$ rotations. The SU(3) chiral field in eq. (3.1) is constructed by using the trivial embedding [28]:

$$U^{\gamma_5} = \begin{pmatrix} U^{\gamma_5}_{\mathrm{SU}(2)} & 0 \\ 0 & 1 \end{pmatrix}, \tag{3.4}$$

where it contains the chiral field SU(2) as a subgroup: $\mathrm{SU}(2)_{\mathrm{flavor}} \otimes \mathrm{SU}(2)_{\mathrm{spin}} \otimes \mathrm{U}(1)_Y \otimes \mathrm{U}(1)_{Y_R}$. Here, Y and Y_R denote the hypercharge and right hypercharge, respectively.

The SU(2) one-particle Dirac Hamiltonian is defined as:

$$h(U) = \gamma_4\gamma_k\partial_k + \gamma_4 M U^{\gamma_5}_{\mathrm{SU}(2)} + \gamma_4\bar{m}, \tag{3.5}$$

where the strange part is obtained by replacing the chiral field by unity, i.e., $U^{\gamma_5} \to 1$. The eigenfunctions and eigenenergies are obtained by diagonalizing $h(U)$:

$$h(U)\psi_n(\boldsymbol{r}) = E_n\psi_n(\boldsymbol{r}), \quad h(1)\psi_{n^0}(\boldsymbol{r}) = E_{n^0}\psi_{n^0}(\boldsymbol{r}). \tag{3.6}$$

The Dirac spectrum E_n consists of the upper and lower Dirac continuum, which are polarized by the pion mean field from the free Dirac spectrum E_{n^0}, and the bound state level energy (or valence quark energy E_v), which emerges when the chiral field is sufficiently strong.

To compute properties such as the mass, spin and electromagnetic properties in the baryonic sector, it is necessary to evaluate the corresponding correlation function with a pion background field. This is done by performing the functional integral described in eq. (3.1). Having integrated the fermionic fields, we obtain the fermionic determinant. The bosonic field can only be solved approximately by using the saddle-point approximation, which holds in the large N_c approximation. In this approach, the result is determined by the integrand evaluated in the classical mesonic configuration. It is important to note that quantum fluctuations are suppressed in the $1/N_c$ expansion [27].

The classical configuration of the pion field $P_{\mathrm{cl}}(r)$ is obtained by solving the following saddle point equation:

$$\left.\frac{\delta S_{\mathrm{eff}}}{\delta P(r)}\right|_{P(r)=P_{\mathrm{cl}}(r)} = 0, \tag{3.7}$$

which yields

$$M_{\mathrm{sol}} = N_c E_{\mathrm{val}} + E_{\mathrm{sea}}, \tag{3.8}$$

where $N_c E_{\mathrm{val}}$ denote the N_c valence-quark (level-quark) contribution, and E_{sea} represents the sum of the negative Dirac continuum energy with the vacuum energy subtracted. This quantity is logarithmically divergent and requires a regularization. The specific regularization functions employed are provided in appendix A.

JHEP05(2024)173

3.2 Collective quantization

The classical soliton does not have the well-defined momentum and spin-flavor quantum numbers. To restore the corresponding symmetries, we introduce translational and rotational zero modes. These modes allow us to replace the functional integral over the mean field U in the presence of a background pion field with the integrals over the center of mass (CM) coordinates $\boldsymbol{X}$ and the rotational matrix R in flavor space:

$$\int \mathcal{D}U\mathcal{F}[U(\boldsymbol{x})] \to \int d^3\boldsymbol{X} \int \mathcal{D}R\,\mathcal{F}\left[TRU_{\rm cl}(\boldsymbol{x})R^\dagger T^\dagger\right], \tag{3.9}$$

where the unitary transformation T represents the translational symmetry. It is important to note that both the CM coordinates $\boldsymbol{X}(t)$ and the rotation matrix $R(t)$ depend weakly on time. The translational zero modes endow the classical soliton with the momentum, while the rotational zero modes furnish it with the spin-flavor quantum numbers. The slow rotation and displacement of the soliton give rise to kinetic corrections that are suppressed in the $1/N_c$ expansion. When considering a baryon in the Breit frame (i.e., $\boldsymbol{P} = (\boldsymbol{p}' + \boldsymbol{p})/2 = 0$), the translational kinetic correction does not contribute to the GFFs. Therefore, in this study we focus on the rotational zero modes to order of $\Omega \sim 1/N_c$ and the translational ones to the zeroth order. Having performed the collective quantization, we obtain the collective Hamiltonian:

$$H_{\rm coll} = M_{\rm sol} + \frac{1}{2I_1}\sum_{i=1}^{3}\hat{J}_i^2 + \frac{1}{2I_2}\sum_{p=4}^{7}\hat{J}_p^2, \tag{3.10}$$

where I_1 and I_2 represent the moments of inertia, and their explicit expressions can be found in appendix A. The hedgehog symmetry of the mean field implies that baryon states emerge with the selection rules: $\boldsymbol{J} + \boldsymbol{T} = 0$ and $Y_R = N_c/3$. Consequently, diagonalizing $H_{\rm coll}$, we derive the rotational wave function for a baryon with spin and flavor indices:

$$\Psi^{(\mu)}_{(YTT_3)(Y_RJJ_3)}(R) = \sqrt{\dim(\mu)}(-1)^{J_3-Y_R/2}D^{(\mu)*}_{(YTT_3)(Y_RJ-J_3)}(R), \tag{3.11}$$

where $D^{(\mu)}_{ab}$ denotes the SU(3) Wigner D function with the corresponding SU(3) representation μ.

3.3 Effective EMT operator

Now we are in a position to derive the effective EMT operator. Given a global symmetry, a conserved current can be derived by the Nöther theorem. However, a non-conserved current such as the flavor nonsinglet EMT current in QCD can be constructed, guided by the singlet EMT current. The effective operator corresponding to the flavor nonsinglet EMT current in QCD can be obtained from the instanton vacuum, which can be coherently adapted to effective quark-gluon dynamics (see figure 1).

3.3.1 EMT current from the global symmetry

This effective dynamics (3.1) includes two degrees of freedom: the dynamical quark and the pion field. In the systematic treatment, i.e. the dilutness of the instanton liquid and the

JHEP05(2024)173

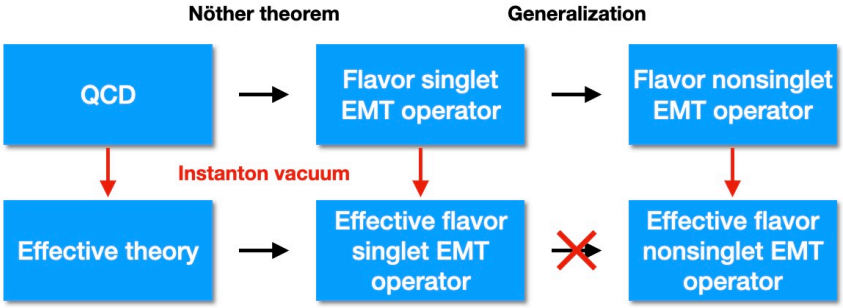

Figure 1. The logical chain that the effective operator derived from the QCD instanton vacuum must be used in the study of flavor-decomposed GFFs is drawn.

$1/N_c$ expansion, all gauge-dependent parts are integrated out through the instanton vacuum. Using the effective action derived from QCD, one can easily obtain a conserved quantity such as the EMT current from the Nöther theorem. The expression for the EMT current in Minkowski space is written as follows [48]:

$$T^{\mu\nu}_{\chi=0}(x) = \frac{i}{4}\bar{\psi}(x)\gamma^{\{\mu}\overleftrightarrow{\partial}^{\nu\}}\lambda_0\psi(x), \tag{3.12}$$

where λ_χ are the SU(3) Gell-Mann matrices with the flavor singlet $\lambda_0 = \mathrm{diag}(1,1,1)$ Gell-Mann matrix. Since there is a kinetic term only for the quarks in the effective action, it is obvious to have the EMT operator with the ordinary derivative. In any models, such as the bag model [79], it is also possible to derive a similar EMT operator without explicit connection to the QCD operator.

As shown in eq. (3.12), it is no longer possible to distinguish between the quark and gluon parts of the EMT current, since the gluon degrees of freedom are absent in the effective action. Thus, this effective operator should be understood as a total (quark+gluon) contribution:

$$T^{\mu\nu}_q(x) + T^{\mu\nu}_g(x)\ [\mathrm{QCD}] \xrightarrow{\mathrm{eff}} T^{\mu\nu}_{\chi=0}(x)\ [\mathrm{Eq.}\ (3.12)]. \tag{3.13}$$

We briefly discuss the various sum rules in QCD. The nucleon momentum and spin sum rules are satisfied by the sum of the quark and gluon contributions

$$\sum_{a=q,g} A^a_N(0) = A_N(0) = 1, \quad \sum_{a=q,g} J^a_N(0) = J_N(0) = 1/2, \quad [\mathrm{QCD}]. \tag{3.14}$$

In addition, the nucleon matrix element of the trace part of the EMT current is normalized to the nucleon mass in QCD in the forward limit:

$$\sum_{a=q,g} \frac{\langle N|T^\mu_{a,\mu}|N\rangle}{2M_N} = M_N A_N(0), \quad \text{with} \quad T^\mu_{q,\mu} = O(m_q), \quad [\mathrm{QCD}]. \tag{3.15}$$

This indicates that the nucleon mass mainly comes from the gluon component of the EMT current, due to the trace anomaly. Similar to the momentum and spin sum rules, the von Laue condition is known as the normalization of the stress tensor, which is closely related to the conservation of the EMT current:

$$\sum_{a=q,g} \int d^3r\ p^a_N(r) = 0, \quad \sum_{a=q,g} \bar{c}^a_N(t) = 0, \quad [\mathrm{QCD}]. \tag{3.16}$$

As a result, the sum of both the quark and the gluon yields the correct sum rules in QCD.

JHEP05(2024)173

In the effective theory, as explained in eq. (3.13), the dynamical quark (+ background pion mean field) alone accounts for the internal dynamics of the nucleon. For example, the momentum and spin sum rules are given only in terms of the quark degrees of freedom (3.14)

$$\sum_{q=u,d,\ldots} A_N^q(0) = A_N(0) = 1, \qquad \sum_{q=u,d,\ldots} J_N^q(0) = J_N(0) = 1/2, \quad \text{[Eq. (3.12)]}. \tag{3.17}$$

the trace anomaly (3.15) is also expressed in terms of the dynamical quarks, which are effectively dressed by gluons:

$$\frac{\langle N|T^\mu_{\chi=0,\mu}|N\rangle}{2M_N} = M_N \sum_{q=u,d,\ldots} A_N^q(0), \quad \text{with} \quad T^\mu_{\chi=0,\mu} = T^{00}_{\chi=0}, \quad \text{[Eq. (3.12)]}. \tag{3.18}$$

Here, we have used the fact that the spatial part of the EMT current vanishes in the forward limit, i.e. $\hat{T}^{ii}_{\chi=0} = 0$. This relation holds true only if the equation of motion of the pion fields (3.7) is satisfied [36, 48]. Owing to the hedgehog symmetry of the self-consistent pion field, one can generalize it to the spatial ij-component of the EMT in the forward limit

$$\frac{i}{2}\bar{\psi}(x)\gamma^i\partial^j\psi(x) = \delta^{ij} f, \quad \text{with} \quad f = 0. \tag{3.19}$$

Interestingly, eq. (3.19) leads to the von Laue condition (see also ref. [48])

$$\sum_{a=q,g} \int d^3r\; p_N^a(r) = 0 \xrightarrow{\text{eff}} \sum_q \int d^3r\; p_N^q(r) = 0, \quad \text{[Eq. (3.12)]}, \tag{3.20}$$

and the null result of the $\bar{c}$ form factor, induced by the conservation of the EMT current,

$$\sum_{a=q,g} \bar{c}_N^a(t) = 0 \xrightarrow{\text{eff}} \sum_q \bar{c}_N^q(t) = 0, \quad \text{[Eq. (3.12)]}. \tag{3.21}$$

As a result, using the flavor-singlet EMT current derived from the global symmetry (3.12), we have succeeded in satisfying all QCD sum rules by means of the dynamical quark and pion fields in the effective theory.

So far, we have discussed the flavor-singlet EMT current. Since we aim at examining the quark flavor decomposition of the GFFs, we need to construct the effective flavor-triplet and -octet EMT currents by introducing the flavor SU(3) Gell-Mann matrices:

$$T^{\mu\nu}_\chi(x) = \frac{i}{4}\bar{\psi}(x)\gamma^{\{\mu}\overleftrightarrow{\partial}^{\nu\}}\lambda_\chi\psi(x). \tag{3.22}$$

Having employed eq. (3.22), we already performed the flavor decomposition of the GFFs [80, 81]. It was also implemented in refs. [82–84].

Strictly speaking, it is only possible to derive the flavor-singlet EMT current (3.12) as a Nöther current. This means that there is no proper way for deriving the flavor-triplet and -octet EMT currents in the effective theory. Thus, we are not able to guarantee that the current given in eq. (3.22) is consistent with the effective quark-gluon dynamics. Consequently, the only way to construct the currents is that starting from the QCD nonsinglet EMT currents we derive the corresponding effective operator from the QCD instanton vacuum. By doing that, we preserve the effective quark-gluon dynamics.

JHEP05(2024)173

3.3.2 EMT current from QCD instanton vacuum

In the systematic expansion (expansions in $1/N_c$ and dilutness of the instanton liquid), the QCD gluon operator can be converted into the effective quark operators in the effective theory [25, 26]. Using this method, we are able to construct the effective operators corresponding to the QCD operators consistently and systematically. Moreover, the low-energy theorems of QCD such as the chiral anomaly and the trace anomaly are correctly satisfied [26].

The chiral-even twist-2 local operator is generated by expanding the non-local vector current, which measures the vector GPDs, with respect to the space-time distance

$$\begin{aligned} O_q^{\mu\nu_1\ldots\nu_n} &:= \bar{\psi}(x)\gamma^{\{\mu}\overleftrightarrow{D}^{\nu_1}\overleftrightarrow{D}^{\nu_2}\ldots\overleftrightarrow{D}^{\nu_n\}}\lambda_\chi\psi(x) - \text{traces}, \\ O_g^{\mu\nu_1\ldots\nu_n} &:= -F^{\{\mu\rho,a}\overleftrightarrow{D}^{\nu_1}\ldots\overleftrightarrow{D}^{\nu_{n-1}}F_\rho^{\nu_n\},a} - \text{traces}. \end{aligned} \tag{3.23}$$

For example, the first and second Mellin moments of the GPDs are known as the leading-twist electromagnetic form factors and GFFs, respectively. The corresponding local currents are given by

$$\begin{aligned} J_\chi^\mu &= \bar{\psi}(x)\gamma^\mu\lambda_\chi\psi(x), \\ \bar{T}_\chi^{\mu\nu} &= \frac{i}{4}\bar{\psi}(x)\gamma^{\{\mu}\overleftrightarrow{D}^{\nu\}}\lambda_\chi\psi(x) - \text{traces}, \qquad \bar{T}_g^{\mu\nu} = -\frac{1}{2}F^{\{\mu\rho,a}F_\rho^{\nu\},a} - \text{traces}. \end{aligned} \tag{3.24}$$

In ref. [25], it was shown that in the twist-2 local operators the effect of the instanton field (gauge field in the covariant derivative) is always of order $(M\bar{\rho})^2$. Thus, when working on leading order in $(M\bar{\rho})$, it is consistent to keep only the ordinary derivative part [order unity $\sim O(1)$] in the twist-2 quark operators

$$\begin{aligned} &\bar{\psi}(x)\gamma^{\{\mu}\overleftrightarrow{D}^{\nu_1}\overleftrightarrow{D}^{\nu_2}\ldots\overleftrightarrow{D}^{\nu_n\}}\lambda_\chi\psi(x) - \text{traces} \\ &\qquad\xrightarrow{\text{eff}} \frac{i}{4}\bar{\psi}(x)\gamma^{\{\mu}\overleftrightarrow{\partial}^{\nu_1}\overleftrightarrow{\partial}^{\nu_2}\ldots\overleftrightarrow{\partial}^{\nu_n\}}\lambda_\chi\psi(x) - \text{traces}, \end{aligned} \tag{3.25}$$

and to set the twist-2 gluon operators by zero:

$$-F^{\{\mu\rho,a}\overleftrightarrow{D}^{\nu_1}\ldots\overleftrightarrow{D}^{\nu_{n-1}}F_\rho^{\nu_n\},a} - \text{traces} \quad\xrightarrow{\text{eff}}\quad 0 \quad + \quad O(M^2\bar{\rho}^2). \tag{3.26}$$

With this parametric order $O(1)$ in the expansion with respect to the packing fraction, we then have the following EMT operators for the effective theory:

$$\bar{T}_\chi^{\mu\nu}(x) = \frac{i}{4}\bar{\psi}(x)\gamma^{\{\mu}\overleftrightarrow{\partial}^{\nu\}}\lambda_\chi\psi(x) - \text{traces}, \quad \bar{T}_g^{\mu\nu}(x) = 0. \tag{3.27}$$

Consequently, this method for deriving the effective operators validates the use of the ordinary derivative operator with trace subtracted. For the purpose of the flavor decomposition, we will use the twist-2 operator (3.27) derived from the QCD, instead of the eq. (3.22). The key difference lies in the subtraction of traces (or twist classification).

For the twist-3 part, the gauge-dependent parts in the covariant derivative lead to spin-flavor dependent quark operators to parametric order $O(1)$. The contributions from these operators have been found to be crucial for satisfying the QCD equation of motion, as discussed in a recent study [73]. Furthermore, they have a significant influence on the numerical values of the orbital angular momentum and the spin-orbit correlation [74].

JHEP05(2024)173

Similar to the twist-3 part [73], the gauge-field dependent part of the twist-4 operators should be replaced by the spin-flavor dependent quark operators. We expect that this twist-4 EMT current will gain the large gauge field contributions of parametric order $O(1)$. It is also essential to consider the gauge-field dependent part of the twist-4 EMT current such that the QCD equation of motion (3.15) is satisfied, i.e., $T^{\mu}_{q,\mu} = 0$ in the chiral limit. The explicit expression of the twist-4 effective operator is currently under derivation, and will appear elsewhere [85]. In this study we will focus on the leading-twist GFFs by using eq. (3.27).

3.4 Matrix element of the EMT current in the large N_c limit of QCD

The matrix element of the symmetrized EMT current in Euclidean space can be calculated as follows:

$$\begin{aligned}\langle B(p', J_3')|\bar{T}_{\mu\nu,\chi}(0)|B(p, J_3)\rangle &= \lim_{T\to\infty} \frac{1}{Z_{\rm eff}} \mathcal{N}^*(p')\mathcal{N}(p) e^{ip_4 \frac{T}{2} - ip_4' \frac{T}{2}} \int d^3\boldsymbol{x}\, d^3\boldsymbol{y} \\ &\times e^{(-i\boldsymbol{p}'\cdot\boldsymbol{y} + i\boldsymbol{p}\cdot\boldsymbol{x})} \int \mathcal{D}\psi\mathcal{D}\psi^\dagger\mathcal{D}U J_B(\boldsymbol{y}, T/2)\bar{T}_{\mu\nu,\chi}(0) J_B^\dagger(\boldsymbol{x}, -T/2) \exp\left[-S_{\rm eff}\right], \end{aligned} \tag{3.28}$$

where J_B represents the Ioffe-type current consisting of the N_c valence quarks [86] and $\bar{T}_{\mu\nu,\chi}(0)$ denotes the twist-2 EMT current (3.27) derived from the effective chiral theory in Euclidean space. Note that $\mathcal{N}^*(p')\mathcal{N}(p')$ yields the non-relativistic normalization $2M_{\rm sol}$, and the baryon state carries the spin, isospin, and hypercharge quantum numbers $B = \{J, J_3, T, T_3, Y\}$.

To understand the behavior of the GFFs, we need to discuss the large N_c limit of the kinematic variables. The large N_c behavior for the baryon mass is given as $M_B \sim \mathcal{O}(N_c) \sim M_{\rm sol}$. The three-momentum shows $p^k \sim \mathcal{O}(N_c^0)$, and the energy scales as $p^0 \sim \mathcal{O}(N_c^1)$. Therefore, the average momentum and the momentum transfer behaves as

$$\Delta^0 \sim O(N_c^{-1}), \quad \Delta^i \sim O(N_c^0), \quad P^0 \sim O(N_c^1), \quad P^i \sim O(N_c^0). \tag{3.29}$$

In addition, the moments of inertia are given in the following order

$$I_1 \sim \mathcal{O}(N_c^1), \quad I_2 \sim \mathcal{O}(N_c^1). \tag{3.30}$$

Defining the static EMT distribution in the large N_c limit

$$\bar{T}^{\mu\nu}_{\chi}(\boldsymbol{r}, J_3', J_3) = \int \frac{d^3\Delta}{(2\pi)^3 2M_{\rm sol}} e^{-i\boldsymbol{\Delta}\cdot\boldsymbol{r}} \left\langle B(p', J_3')|\bar{T}^{\mu\nu}_{\chi}(0)|B(p, J_3)\right\rangle, \tag{3.31}$$

we obtain the final expressions for the GFFs[1] as the 3D Fourier transforms of the EMT

[1]Instead of using the $A(t)$ form factor, we adopt the 3D multipole form factor $\bar{\mathcal{E}}$, which reveals the clear and natural N_c scaling. This is also true for the electromagnetic form factors. The Sach form factors G_E and G_M exhibit a clearer and more natural N_c scaling than the Pauli and Dirac form factors $F_{1,2}(t)$. These facts are deeply rooted in the non-relativistic nature of the collective nucleon motion in the large N_c limit of QCD.

JHEP05(2024)173

distributions:

$$\begin{aligned}
\bar{\mathcal{E}}^{\chi}_{B}(t)\delta_{J'_3 J_3} &= \frac{1}{M_{\rm sol}}\int d^3 r\, j_0(r\sqrt{-t})\bar{\varepsilon}^{\chi}_{B}(r),\\
\bar{\mathcal{P}}^{\chi}_{B}(t)\delta_{J'_3 J_3} &= \frac{1}{M_{\rm sol}}\int d^3 r\, j_0(r\sqrt{-t})\bar{p}^{\chi}_{B}(r),\\
D^{\chi}_{B}(t)\delta_{J'_3 J_3} &= 4M_{\rm sol}\int d^3 r \frac{j_2(r\sqrt{-t})}{t} s^{\chi}_{B}(r),\\
2S^3_{J'_3 J_3} J^{\chi}_{B}(t) &= 3\int d^3 r \frac{j_1(r\sqrt{-t})}{r\sqrt{-t}}\rho^{\chi}_{J,B}(r),
\end{aligned} \tag{3.32}$$

where the respective distributions $\bar{\varepsilon}^{\chi}_{B}$, $\rho^{\chi}_{J,B}$, s^{χ}_{B}, and $\bar{p}^{\chi}_{B}$ are given by

$$\begin{aligned}
\bar{\varepsilon}^{\chi}_{B}(r) &= \frac{1}{\sqrt{3}}\langle D_{\chi 8}\rangle_B \mathcal{M}(r) - \frac{2}{I_1}\langle D_{\chi i}J_i\rangle_B \mathcal{J}_1(r) - \frac{2}{I_2}\langle D_{\chi a}J_a\rangle_B \mathcal{J}_2(r),\\
\rho^{\chi}_{J,B}(r) &= \langle D_{\chi 3}\rangle_B\left(\mathcal{Q}_0(r) + \frac{1}{I_1}\mathcal{Q}_1(r)\right) - \frac{1}{\sqrt{3}}\langle D_{\chi 8}J_3\rangle_B \frac{1}{I_1}\mathcal{I}_1(r) - \langle d_{ab3}D_{\chi a}J_b\rangle_B \frac{1}{I_2}\mathcal{I}_2(r),\\
s^{\chi}_{B}(r) &= \frac{1}{\sqrt{3}}\langle D_{\chi 8}\rangle_B \mathcal{N}_1(r) - \frac{2}{I_1}\langle D_{\chi i}J_i\rangle_B \mathcal{J}_3(r) - \frac{2}{I_2}\langle D_{\chi a}J_a\rangle_B \mathcal{J}_4(r),\\
\bar{p}^{\chi}_{B}(r) &= \frac{1}{3}\bar{\varepsilon}^{\chi}_{B}(r).
\end{aligned} \tag{3.33}$$

The $\langle\ldots\rangle_B$ denotes the matrix element of the SU($2N_f$) spin-flavor operators between the initial and final rotational wave functions

$$\langle\ldots\rangle_B = \int dR\, \Psi^{(\mu)*}_{(Y'T'T'_3)(Y_R J' J'_3)}(R)\ \ldots\ \Psi^{(\mu)}_{(YTT_3)(Y_R J J_3)}(R). \tag{3.34}$$

The detailed expressions for the distributions $\mathcal{M}$, $\mathcal{J}_1$, $\mathcal{J}_2$, etc. are given in appendix A. In the limit $\chi \to 0$, the results for the flavor singlet EMT distributions [48, 87] are recovered as follows:

$$\begin{aligned}
\bar{\varepsilon}^{0}_{B}(\boldsymbol{r}) &= \mathcal{M}(\boldsymbol{r}), \quad \rho^{0}_{J,B}(\boldsymbol{r}) = -\frac{1}{2I_1}\mathcal{I}_1(\boldsymbol{r}),\\
s^{0}_{B}(\boldsymbol{r}) &= \mathcal{N}_1(\boldsymbol{r}), \quad \bar{p}^{0}_{B}(\boldsymbol{r}) = \frac{1}{4}\mathcal{M}(\boldsymbol{r}).
\end{aligned} \tag{3.35}$$

The integrals of the individual EMT distributions over 3D space satisfy the following relations:

$$\int d^3 r\, \mathcal{M}(\boldsymbol{r}) = \frac{3}{4}M_{\rm sol}, \quad \int d^3 r\, \mathcal{I}_1(\boldsymbol{r}) = -I_1, \tag{3.36}$$

Using eq. (3.36), we find that the mass and AM form factors are properly normalized to its mass [$A_B(0) = 1$] and AM [$J_B(0) = 1/2$]

$$\int d^3 r\, \bar{\varepsilon}^{0}_{B}(\boldsymbol{r}) = \frac{3}{4}M_{\rm sol}, \quad \int d^3 r\, \rho^{0}_{J,B}(\boldsymbol{r}) = 1/2. \tag{3.37}$$

In addition, the first relation in eq. (3.36) results in break down of the von Laue condition:

$$\int d^3 r\, \bar{p}^{0}_{B}(\boldsymbol{r}) = \frac{1}{4}M_{\rm sol}. \tag{3.38}$$

JHEP05(2024)173

The inclusion of the twist-4 contribution restores the von Laue condition. It can be inferred indirectly from the estimation of the EMT distribution using the EMT current (3.12) derived from the Nöther theorem. When we use the EMT current (3.12), we find that the presence of the s quark has no effect on the normalizations of the GFFs and the von Laue condition (see refs. [80, 81]). It is noteworthy that the mass and AM normalizations hold true regardless of the configuration of the pion mean field. However, the von Laue condition is only satisfied when the pion mean field assumes a classical configuration. This emphasizes the importance of considering the dynamical nature of the system when describing properties related to the stress tensor.

Furthermore, while the conserved EMT current ensures the normalization of the total AM, the distinction between intrinsic spin and OAM remains an important issue for careful investigation (see refs. [73, 74]).

4 Numerical results

Before delving into the numerical results for the flavor decompositions of the EMT distributions and form factors, it is crucial to acknowledge the limitations of the current approach. We have made certain assumptions regarding the rotational and translational zero modes, treating them up to corrections of $1/N_c$ and zero, respectively. Additionally, we have considered the flavor SU(3) symmetry where the strange current quark mass, m_s, is set to $m_u = m_d = m_s$. We have previously investigated the impact of m_s on the GFFs and EMT distributions, and found that while these contributions introduce some differences in the octet baryon GFFs, they are ultimately negligible, with m_s corrections approximately 10% [87]. Moreover, if we were to include the m_s corrections in the stress tensor T^{ij}, the von Laue condition would be violated. Consequently, we would have to artificially reconstruct the pressure distribution by solving the differential equation (2.32) in terms of the shear-force distributions. Therefore, in the context of examining flavor structures, it is reasonable to ignore these contributions in order to clearer understand the GFFs and distributions.

4.1 Mass distribution: twist-2 part

As discussed in the previous section, we will discuss the twist-2 mass distribution decoupled from the $\bar{c}$ form factor. By taking the linear combinations of the $\chi = 0, 3, 8$ components of eq. (3.33), we can derive the flavor-singlet, -triplet, and -octet components of the mass distributions of the nucleon. It is important to note that the 3D mass distribution, defined in the instant form quantization at the rest frame, is normalized as follows:

$$\frac{3}{4} A_p^\chi(0) = \frac{1}{M_{\rm sol}} \int d^3r \, \bar{\varepsilon}_p^\chi(r). \tag{4.1}$$

The values of each component $\chi = 0, 3, 8$ for the mass form factors (or normalization of the mass distribution) are listed as follows:

$$\begin{aligned} &A_p^0(0) = 1, \quad A_p^3(0) = 0.25, \quad A_p^8(0) = 0.47, \quad [\,\mathrm{SU(3)}\,] \\ &A_p^0(0) = 1, \quad A_p^3(0) = 0.24 \qquad\qquad\quad [\,\mathrm{SU(2)}\,]. \end{aligned} \tag{4.2}$$

JHEP05(2024)173

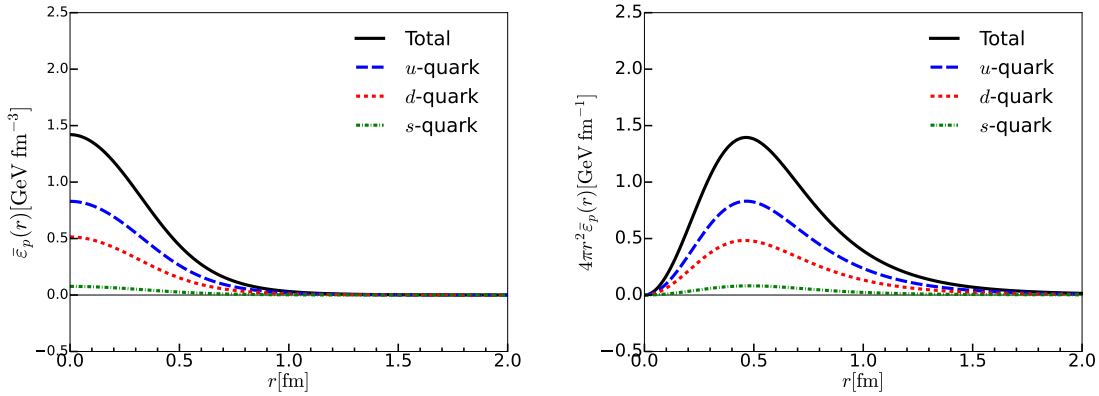

Figure 2. The 3D mass distribution of the proton and its flavor decomposition with the flavor SU(3) symmetry are plotted. The solid (black), long-dashed (blue), short-dashed (red), and dashed-dotted (green) curves denote the total, u-, d-, and s-quark contributions to the mass distributions, respectively.

The proton twist-2 mass distribution, or the flavor-singlet mass distribution $\bar{\varepsilon}_p^0$, is normalized to its mass $3M_{\rm sol}/4$, which ensures that the mass form factor is normalized to $A_p^0(0) = 1$. Since the spin-flavor operator of the flavor-singlet component is proportional to unity, the masses of the octet baryons are all degenerate. It is worth noting that as discussed in eq. (3.27) the gluon contributions to the leading-twist operators are parametrically suppressed with respect to the instanton packing fraction [25, 88], allowing us to consider them negligible at the low normalization point of $\mu \sim 600\,\text{MeV}$. Therefore, the gluon contributions to the leading-twist GFFs can be ignored throughout this study:

$$A_B^g = 0, \quad J_B^g = 0. \tag{4.3}$$

Thus, the normalization of the nucleon mass is solely determined by the quark contributions. Furthermore, we observe that the flavor-triplet mass distribution is smaller than the flavor-singlet one. It suggests that the parametric suppression of the flavor triplet in SU(2) symmetry remains valid in flavor SU(3) symmetry. In addition, the flavor octet component of the mass form factor is approximately half of the singlet component. We can determine the individual quark contributions to the mass distribution of the proton. The left panel of figure 2 shows the 3D mass distribution of the nucleon and its flavor decomposition with the flavor SU(3) symmetry. First, they are kept positive definite at any given r

$$\bar{\varepsilon}_p^{u,d,s}(r) > 0. \tag{4.4}$$

Numerically, we find that the sum of the u- and d-quark contributions, as well as the s-quark contribution, is normalized to $3M_{\rm sol}/4$ when integrated over r. At the origin of the proton, the magnitudes of the mass distributions for the u-, d-, and s-quarks are found to be:

$$\begin{aligned} &\bar{\varepsilon}_p^u(0) = 0.83\ \text{GeV/fm}^3, \quad \bar{\varepsilon}_p^d(0) = 0.51\ \text{GeV/fm}^3, \\ &\bar{\varepsilon}_p^s(0) = 0.08\ \text{GeV/fm}^3. \end{aligned} \tag{4.5}$$

We observe that the u-quark contributions to the mass distribution are approximately twice as large as those of the d-quark for the proton. This can be intuitively understood by considering

JHEP05(2024)173

the number of valence quarks inside the proton. Additionally, the s-quark contribution is approximately 10% of the u-quark contribution. Notably, while the role of the u-quark inside a proton is taken by the d-quark inside a neutron, i.e., $\bar{\varepsilon}^u_p(r) = \bar{\varepsilon}^d_n(r)$, the s-quark contribution remains unchanged, i.e., $\bar{\varepsilon}^s_p(r) = \bar{\varepsilon}^s_n(r)$.

In the right panel of figure 2, we depict the r^2-weighted mass distributions. To quantify how far the mass distributions spread over coordinates space, we introduce the 3D mass radius. Since the total mass radius is independent of the $\bar{c}$ form factor, we unambiguously obtain it in the flavor SU(3) symmetry

$$\langle r^2_{\rm mass}\rangle_p = 0.54 \text{ fm}^2, \tag{4.6}$$

which is equal to the radius in the flavor SU(2) symmetry. It is important to note that, as discussed in refs. [76, 87], the mass radius is smaller than the charge radius.

Next, we consider the individual quark contributions to the proton momentum fraction carried by the quark $A^q_p(0)$. This quantity can be accessed directly from the twist-2 GFF $\mathcal{E}^q_p(0) = \frac{3}{4}A^q_p(0)$ as follows:

$$\begin{aligned} &A^u_p(0) = 0.59, \quad A^d_p(0) = 0.35, \quad A^s_p(0) = 0.06, \quad [\,\text{SU(3)}\,] \\ &A^u_p(0) = 0.62, \quad A^d_p(0) = 0.38, \qquad\qquad\quad [\,\text{SU(2)}\,]. \end{aligned} \tag{4.7}$$

In other words, these numbers can be understood as the second Mellin moments of the PDFs. We list the predictions of the proton momentum fraction carried by the u-, d-, and s-quarks:

$$[\langle x\rangle_u : \langle x\rangle_d : \langle x\rangle_s] = [59\% : 35\% : 6\%]. \tag{4.8}$$

4.2 Angular momentum distribution

By taking the components $\chi = 0, 3, 8$ from equation (3.33), we obtain the flavor-singlet, -triplet, and -octet AMs. While the flavor-singlet AM is appropriately normalized to $J^0_p(0) = 1/2$, given by

$$J^0_p(0) = \int d^3r\, \rho^0_{J,p}(r) = \frac{1}{2}, \tag{4.9}$$

the flavor-triplet and -octet components are not constrained by conserved quantities and are estimated as follows:

$$\begin{aligned} &J^0_p = 0.50, \quad J^3_p = 0.58, \quad J^8_p = 0.22, \quad [\,\text{SU(3)}\,] \\ &J^0_p = 0.50, \quad J^3_p = 0.55, \qquad\qquad [\,\text{SU(2)}\,]. \end{aligned} \tag{4.10}$$

The parametrically large value of the flavor-triplet AM in the flavor SU(2) symmetry is retained in the flavor SU(3) symmetry. Furthermore, the flavor-octet component exhibits the same order of N_c as the flavor-triplet component, but numerically it is approximately a half of its magnitude.

Figure 3 illustrates the individual flavor-decomposed AM distributions inside the proton, utilizing the relations provided in eq. (2.6). Notably, the u- and s-quark distributions exhibit positive values throughout the range of r, while the d-quark distribution is negative. It

JHEP05(2024)173

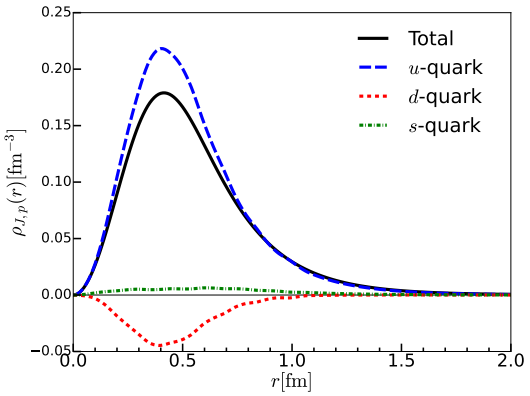

Figure 3. The 3D AM distribution of the nucleon and its flavor decomposition with the flavor SU(3) symmetry are drawn. The solid (black), long-dashed (blue), short-dashed (red), and dashed-dotted (green) curves denote the total, u-, d-, and s-quark contributions to the AM distributions, respectively.

implies that the polarization of the s-quark aligns parallel to that of the u-quark, whereas the d-quark polarization is arranged in the opposite direction to that of the u-quark. When these 3D AM distributions are integrated over r, the resulting values are shown below:

$$\begin{aligned} &J_p^u = 0.52, \quad J_p^d = -0.06, \quad J_p^s = 0.04, \quad [\,\mathrm{SU}(3)\,] \\ &J_p^u = 0.53, \quad J_p^d = -0.03, \qquad\qquad\quad [\,\mathrm{SU}(2)\,]. \end{aligned} \tag{4.11}$$

As expected, the total AM is mostly carried by the u-quark, whereas the d-quark and s-quark give only minor contributions. These results are in line with the predictions from the SU(2) version of the χQSM [80] and are compatible with findings from lattice QCD simulations [89]. A comprehensive analysis of the scale evolution of the AM form factors can be found in refs. [90, 91].

In comparison with the results obtained from the SU(2) χQSM [48, 80, 92], we observe that while the contribution of the u-quark to the total AM remains nearly unchanged, the polarization of the d-quark contribution is slightly enhanced. This suggests that the s quark is polarized in the opposite direction to the d quark, effectively canceling each other out and keeping the total AM at 1/2. Interestingly, the magnitude of the s quark contribution to the total AM is nearly equal to that of the d quark contribution. However, a non-trivial question arises regarding the decomposition of AM into spin and OAM. According to the Ji's relation [17], the total AM can be expressed as the sum of the intrinsic spin and the OAM:

$$J = \frac{1}{2}\sum_q \Delta q + \sum_q L^q + J_g, \quad J_g = 0, \tag{4.12}$$

where we focus on the quark contributions, since the gluon contributions are parametrically suppressed in the QCD instanton vacuum [25, 26]. In the χQSM, the antisymmetric part of the $0k$ component of the Ji's EMT current captures the spin of the s-wave quarks, while the non-symmetric part accounts for the quark AM with OAM $L = 1$. This implies that the static quark spin and the relativistic motion of the quark explain the intrinsic spin and

JHEP05(2024)173

OAM, respectively. Remarkably, we find that 50% of the flavor-singlet AM is due to the relativistic motion of the quarks inside the nucleon:

$$\frac{1}{2} = \frac{1}{2}\sum_q \Delta q + \sum_q L^q = 0.23 + 0.27. \tag{4.13}$$

It is worth noting that the effect of corrections due to the strange quark mass (m_s) on the AM decomposition has been estimated in ref. [87] and found to be negligible, with only a few percent effect on the proton. Furthermore, in the χQSM, the validity of Ji's relation for the flavor singlet component has been analytically proven in refs. [48, 93], even in the presence of flavor SU(3) symmetry breaking [87]. However, a careful treatment is required to study the separate contributions of the quark flavors to the OAM and the intrinsic spin for the following two reasons: different UV divergence patterns between the total angular momentum and the separate spin and the OAM [94]; lack of knowledge of the proper matching between the QCD operator and the twist-3 effective operator [73].

4.3 Mechanical properties: twist-2 part

The ij component of the EMT is related to the pressure and shear-force distributions by the 3D Fourier transform and provides crucial information for understanding the stability conditions of the nucleon. To fully interpret these mechanical properties, knowledge of both the $\bar{c}$ and D term form factors is required. A well-known stability condition, known as the von Laue condition, arises from the conservation of the EMT current. Similar to the normalization of the mass and spin of the baryon, the von Laue condition serves as a normalization condition for the stress tensor.

First, if we use the EMT current (3.12) derived from the Nöther theorem, all the quark and gluon parts are effectively included in eq. (3.12). Using this effective current, the analytical proof of the global stability condition was carried out in ref. [48], which considers only u and d quarks. Importantly, this result holds even in the case of flavor SU(3) symmetry, since the expression for the SU(2) isoscalar pressure distribution [48, 80, 87] coincides with that of the SU(3) flavor-singlet pressure distribution [87]:

$$\int d^3r\, p_p^{u+d+s}(r) = 0. \tag{4.14}$$

However, as emphasized in section 3.3, there is no proper way of constructing the effective flavor-triplet and -octet EMT currents by a global symmetry. Thus, instead of using (3.22), we will adopt the effective operator (3.27) derived from the QCD instanton vacuum and concentrate on the twist-2 part. The integral of the twist-2 part of the pressure distribution over r is not zero:

$$\int d^3r\, \bar{p}_p^{u+d+s}(r) = \frac{1}{4}M_N, \quad \int d^3r\, \hat{p}_p^{u+d+s}(r) = -\frac{1}{4}M_N. \tag{4.15}$$

Compared to eq. (4.14), the amount of energy $\frac{1}{4}M_N$ in eq. (4.15) leaks away to the twist-4 quark and gluon part, of which the amount is 1/3 times the normalization for the twist-2 energy distribution. Obviously, there is no role for the $\bar{c}$ form factor in the flavor-singlet twist-2 and twist-4 pressure distributions. On the other hand, as discussed in eq. (2.29), each quark

JHEP05(2024)173

contribution to the von Laue condition is due to the $\bar{c}$ form factor, which is beyond the scope of the present work. What we can at least discuss is the flavor decomposition of the twist-2 part

$$\int d^3r\, \bar{p}^u_p(r) = \frac{1}{4} M_N A^u_p(0), \quad \int d^3r\, \bar{p}^d_p(r) = \frac{1}{4} M_N A^d_p(0),$$
$$\int d^3r\, \bar{p}^s_p(r) = \frac{1}{4} M_N A^s_p(0). \tag{4.16}$$

They are only proportional to the $A^q_p(0)$ form factors, which in turn are canceled out by a part of the twist-4 part.

Unlike the pressure distribution, the shear-force distribution is the off-diagonal part of the EMT. Thus, regardless of the twist classification, we can extract the D-term form factor from the shear-force distribution. For the quark part, we obtain the flavor singlet, triplet, and octet D-term form factors by Fourier transform of the shear-force distributions:

$$\begin{aligned} &D^0_p(0) = -2.531, \quad D^3_p(0) = 0.063, \quad D^8_p(0) = -0.697, \quad [\,\mathrm{SU}(3)\,] \\ &D^0_p(0) = -2.531, \quad D^3_p(0) = 0.295, \qquad\qquad\qquad\quad [\,\mathrm{SU}(2)\,]. \end{aligned} \tag{4.17}$$

Note that the gluon contributions to the D-term form factor are suppressed at low normalization points

$$D^g = 0. \tag{4.18}$$

Burkert *et al.* [95] analyzed the experimental data on DVCS, and extracted the D-term form factor assuming the large N_c while neglecting s-quark contributions. In the flavor SU(2) sector, the isovector component of the D-term is parametrically small in the large N_c, but we find that it is numerically non-negligible. On the other hand, in the flavor SU(3) case, the flavor-triplet D-term is almost zero, i.e., $D^3_p \sim 0$. This suggests that the large N_c assumption is more appropriate for the flavor SU(3) sector. In lattice QCD simulations [96, 97] in the flavor SU(2) sector, the value of the isovector D-term is found to be very small. However, lattice results suffer from substantial uncertainties, leaving the sign of the isovector D-term undetermined. Very recently, the lattice simulation [98] performed in the flavor SU(3) sector predicts an almost zero value of the isovector D-term form factor, which is consistent with the prediction of the current work.

We obtain the flavor-decomposed pressure and shear-force distributions by linearly combining the $\chi = 0, 3, 8$ components. The resulting distributions are depicted in figure 4. The values of the flavor-decomposed pressures at the center of the proton are given by

$$\bar{p}^u_p(0) = 0.28\ \mathrm{GeV/fm}^3, \quad \bar{p}^d_p(0) = 0.17\ \mathrm{GeV/fm}^3,$$
$$\bar{p}^s_p(0) = 0.03\ \mathrm{GeV/fm}^3. \tag{4.19}$$

As discussed in eq. (2.27), the pressure distribution is three times smaller than the energy distribution, which is reflected in the numbers listed in (4.5) and (4.19). The dominance of the u-quark in the central region is evident, as valence quarks tend to cluster around the core. To satisfy the von Laue condition, the total pressure distribution p^{u+d+s} must have at least one nodal point. However, the twist-2 pressure distribution for each quark is always

JHEP05(2024)173

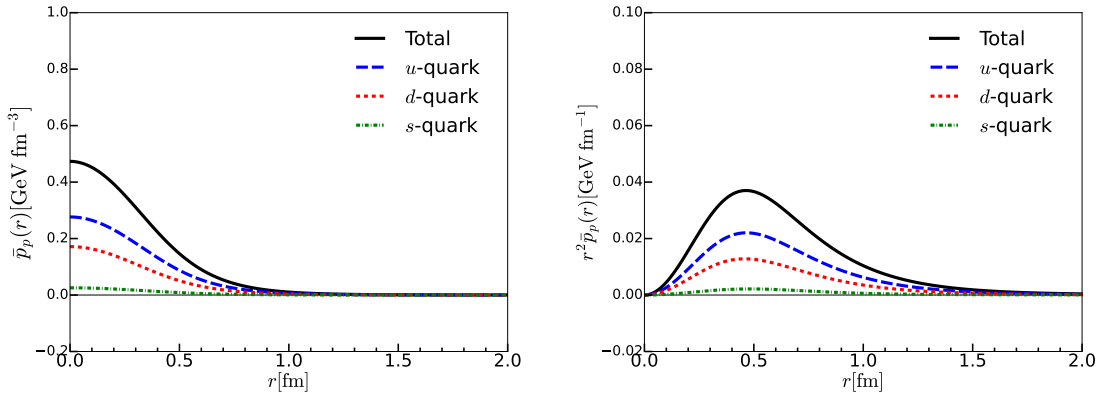

Figure 4. The 3D pressure distribution of the nucleon and its flavor decomposition with SU(3) symmetry are plotted. The solid (black), long-dashed (blue), short-dashed (red), and dashed-dotted (green) curves denote the total, u-, d-, and s-quark contributions to the pressure distributions, respectively.

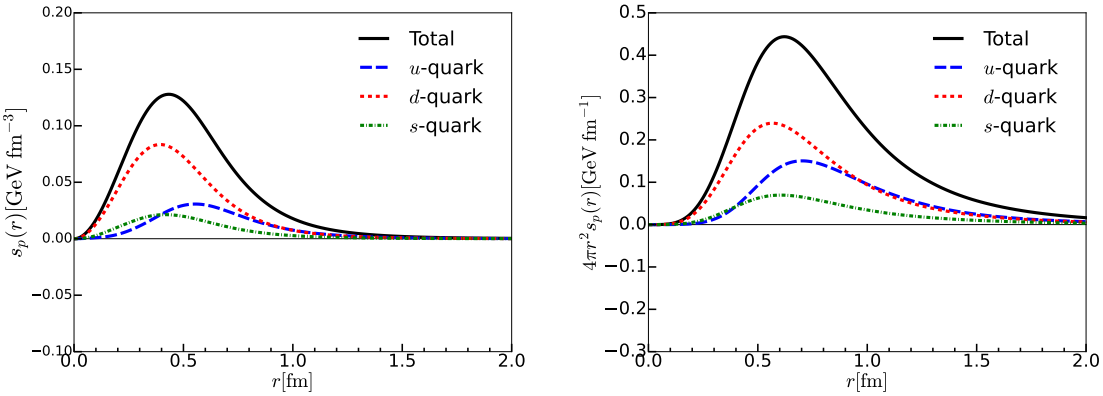

Figure 5. The shear-force distribution of the nucleon and its flavor decomposition with the flavor SU(3) symmetry are drawn. The solid (black), long-dashed (blue), short-dashed (red), and dashed-dotted (green) curves denote the total, u-, d-, and s-quark contributions to the pressure distributions, respectively.

positive over r [see (4.4)]. This implies that it has no nodal point at all. As a result, since the twist-2 part shows only the repulsive force, we can expect that the twist-4 part would provide attractive forces to stabilize the nucleon system.

In figure 5, the flavor-decomposed shear-force distributions are drawn. All the flavor-decomposed shear-force distributions have been determined to be positive throughout the range of r. This positive definiteness of the shear force distribution, $\sum_q s_p^q(r) > 0$, leads to the inequality [24, 48, 75, 77]:

$$\frac{2}{3}s_p(r) + p_p(r) > 0, \tag{4.20}$$

which comes from the equilibrium equation (2.33) relating the pressure distribution to shear-force one.

JHEP05(2024)173

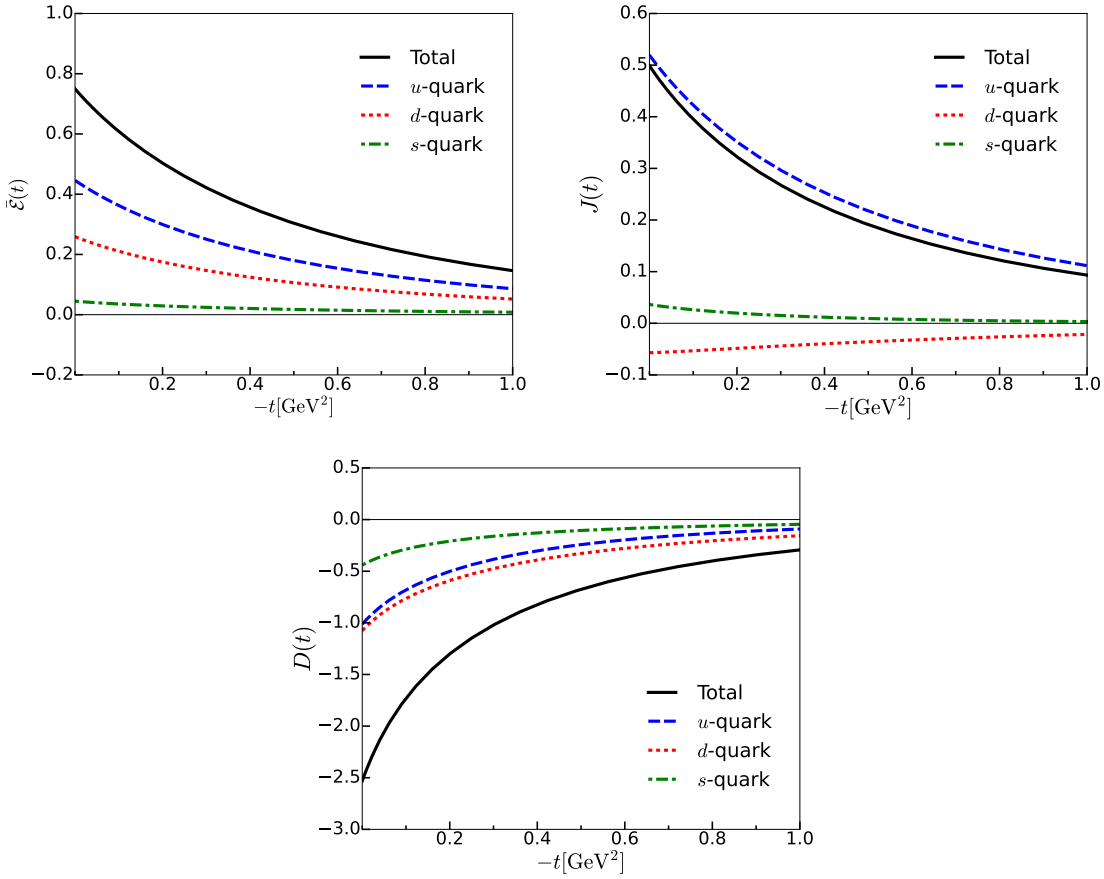

Figure 6. The flavor-decomposed gravitational form factors of the proton are drawn. The solid (black), long-dashed (blue), short-dashed (red), and dashed-dotted (green) curves denote the total, u-, d-, and s-quark contributions to the GFFs, respectively.

4.4 Flavor-decomposed GFFs of the proton

We are now in a position to examine the t-dependence of the nucleon GFFs in the flavor SU(3) symmetry. By performing a 3D Fourier transform of the EMT distributions, we obtain the GFFs, which are depicted in figure 6. As discussed in the previous subsection, we have observed that the s-quark contributions to the A and J form factors are marginal. However, the s-quark's influences on the D form factor is found to be non-negligible. Consequently, the s-quark plays an important role in the mechanical interpretation of the proton. For additional insights into the contributions of valence and sea quarks to the GFFs, refer to ref. [81].

4.5 SU(3) spin-flavor sturcture and the hyperon GFFs

In the large N_c limit of QCD, the relation between the lowest-lying baryons can be understood in a model-independent manner using spin-flavor symmetry. While the GFFs in the flavor SU(2) symmetry were investigated in ref. [56], we aim to extend this analysis to the flavor SU(3) sector in our current work. The chiral soliton approach describes the spin-flavor symmetry using collective operators. The matrix elements of these operators, which are listed in tables 2 and 3, provide insights into the spin-flavor structure.

JHEP05(2024)173

B	$A_B^u(0)$	$A_B^d(0)$	$A_B^s(0)$	$J_B^u(0)$	$J_B^d(0)$	$J_B^s(0)$	$D_B^u(0)$	$D_B^d(0)$	$D_B^s(0)$
p	0.595	0.345	0.060	0.520	−0.057	0.036	−1.014	−1.076	−0.441
n	0.345	0.595	0.060	−0.057	0.520	0.036	−1.076	−1.014	−0.441
Λ	0.339	0.339	0.321	0.055	0.055	0.390	−0.960	−0.960	−0.611
Σ^+	0.595	0.060	0.345	0.520	0.036	−0.057	−1.014	−0.441	−1.076
Σ^0	0.327	0.327	0.345	0.278	0.278	−0.057	−0.727	−0.727	−1.076
Σ^-	0.060	0.595	0.345	0.036	0.520	−0.057	−0.441	−1.014	−1.076
Ξ^0	0.345	0.060	0.595	−0.057	−0.036	0.552	−1.076	−0.441	−1.014
Ξ^-	0.060	0.345	0.595	−0.036	−0.057	0.520	−0.441	−1.076	−1.014

Table 1. Flavor-decomposed gravitational form factors for the octet baryons.

Utilizing the matrix elements of the spin-flavor operators, we establish the following spin-flavor relations in the flavor SU(3) symmetry:

- The flavor-singlet GFFs for the octet baryons are degenerate.
- The flavor-triplet GFFs are propotional to the isospin projection T_3, i.e., $F_B^3 \propto T_3$. Consequently, we find the relations:

$$\sum_{B\in\text{octet}} F_B^3 = 0, \quad \sum_{B=p,n} F_B^3 = 0, \qquad \sum_{B=\Sigma^+,\Sigma^0,\Sigma^-} F_B^3 = 0, \quad \sum_{B=\Xi^0,\Xi^-} F_B^3 = 0. \tag{4.21}$$

- The flavor-octet GFFs for the iso-multipolets are degenerate. Additionally, we obtain:

$$\sum_{B\in\text{octet}} F_B^8 = 0, \quad \sum_{B=\Lambda,\Sigma} F_B^8 = 0. \tag{4.22}$$

Remarkably, our numerical calculations confirm that these spin-flavor relations are indeed satisfied; see table 1.

Figure 7 displays the $\bar{\mathcal{E}}^{0,3,8}$ form factors for the octet baryons. Firstly, we observe that the $\bar{\mathcal{E}}^0$ form factors for the baryon octet are clearly degenerate, which arises from the absence of m_s corrections. Introducing these corrections would break the degeneracy among the mass form factors $\bar{\mathcal{E}}$ for the baryon octet, as discussed in ref. [87]. Secondly, the $\bar{\mathcal{E}}^3$ form factors for the baryon octet are proportional to the third component of the isospin, denoted as $\propto T^3$. This implies that $\bar{\mathcal{E}}^3_{\Lambda^0,\Sigma^0}(t) = 0$. Additionally, the sums of the $\bar{\mathcal{E}}^3$ form factors for the iso-multiplets yield zero. Lastly, the $\bar{\mathcal{E}}^8$ form factors for the iso-multiplet members are degenerate. Interestingly, we derive the following relations:

$$\sum_{B=N,\Xi} \bar{\mathcal{E}}_B^8 = 0, \quad \sum_{B=\Lambda,\Sigma} \bar{\mathcal{E}}_B^8 = 0. \tag{4.23}$$

Consequently, table 1 provides the flavor-decomposed GFFs. Notably, the u-, d-, and s-quarks carry almost equally the momentum fraction of the Λ^0 and Σ^0 baryons. This follows from the nearly vanishing values of the flavor-octet components $A^8_{\Sigma^0,\Lambda^0}(0) \sim 0$. Comparing it with the

JHEP05(2024)173

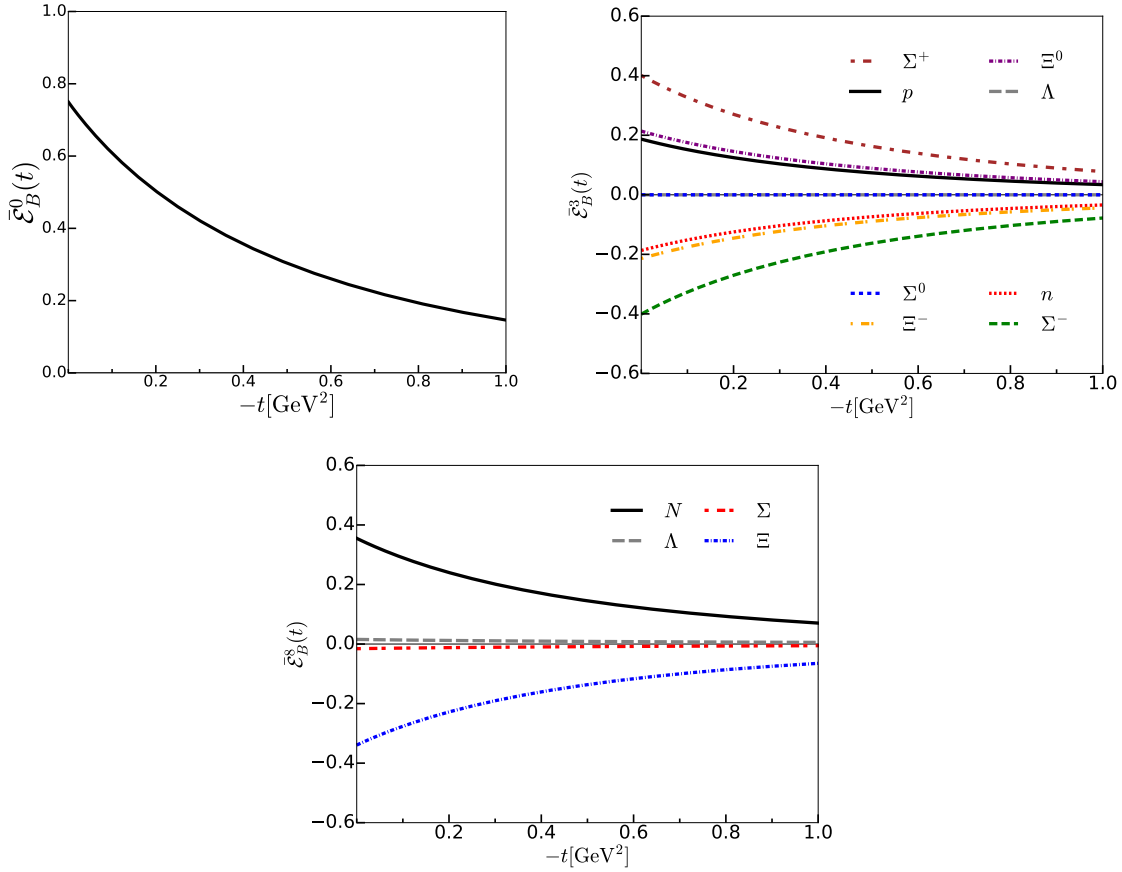

Figure 7. Flavor-singlet, -triplet, and -octet $\bar{\mathcal{E}}$ form factors for the octet baryons are drawn.

proton, the Σ^+ baryon contains one less d-quark and one additional s-quark in the valence level, leading to an exchange in the roles of $\bar{\mathcal{E}}^d$ and $\bar{\mathcal{E}}^s$ between the proton and the Σ^+ baryon. Similar tendencies are observed for the Σ^-, Ξ^0, and Ξ^- baryons.

Figure 8 illustrates the $J^{0,3,8}$ form factors for the octet baryons. Firstly, we observe that the J^0 form factors for the octet baryons are also degenerate. However, this degeneracy can be lifted by considering m_s corrections, as discussed in ref. [87]. Secondly, the J^3 form factor for the octet baryons is once again proportional to T^3, resulting in null results for the Σ^0 and Λ^0 baryons. While the octet components J^8 for the iso-multiplet members remain degenerate, we find the following relations:

$$\sum_{B=N,\Xi} J^8_B \neq 0, \qquad \sum_{B=\Lambda,\Sigma} J^8_B = 0. \tag{4.24}$$

Thus, in contrast to the $\bar{\mathcal{E}}^8$ form factors, the angular-momentum form factors have a different flavor structure. In table 1, we provide the flavor-decomposed J form factors. It is interesting to note that the Λ^0 and Σ^0 baryons exhibit different quark contributions despite having the same quark content. This finding is reminiscent of the flavor-decomposed axial charges

JHEP05(2024)173

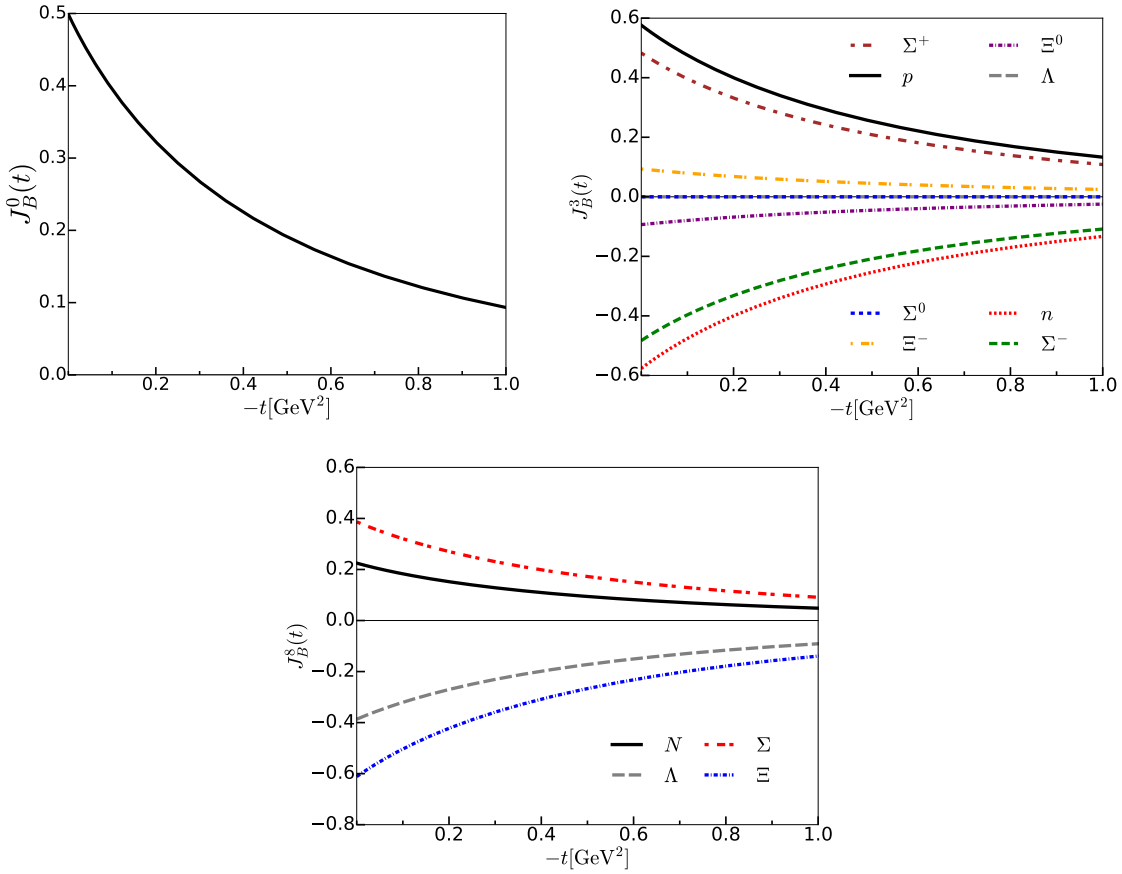

Figure 8. Flavor-singlet, -triplet, and -octet J form factors for the baryon octet are drawn.

presented in ref. [99]:

$$\begin{aligned} \Delta u_{\Lambda^0} &= -0.093, \quad \Delta d_{\Lambda^0} = -0.093, \quad \Delta s_{\Lambda^0} = +0.623, \\ \Delta u_{\Sigma^0} &= +0.384, \quad \Delta d_{\Sigma^0} = +0.384, \quad \Delta s_{\Sigma^0} = -0.332. \end{aligned} \tag{4.25}$$

Thus, we conclude that the spin and OAM of the s-quark in the Λ^0 baryon are strongly polarized, while those in the Σ^0 baryon are relatively weakly polarized, despite both baryons having the same quark content. For the p, n, Σ^+, Σ^-, Ξ^0, and Ξ^- baryons, we can easily obtain the flavor-decomposed $J^q(0)$ form factors by considering the number of valence quarks. For instance, the flavor-decomposed $J^q(0)$ form factors for the Σ^+ baryon are found to be:

$$\begin{aligned} \text{two quarks with the same flavor } (u) \to J^u(0) &= +0.520, \\ \text{one quark } (s) \to J^s(0) &= -0.057, \\ \text{non-valence quark } (d) \to J^d(0) &= +0.036. \end{aligned} \tag{4.26}$$

In figure 9, we present the $D^{0,3,8}$ form factors for the octet baryons. We observe that the $D^0(t)$ form factors for the octet baryons are degenerate, similar to the previous cases. Additionally, the D^3 form factors for the octet baryons are proportional to T^3, following the

JHEP05(2024)173

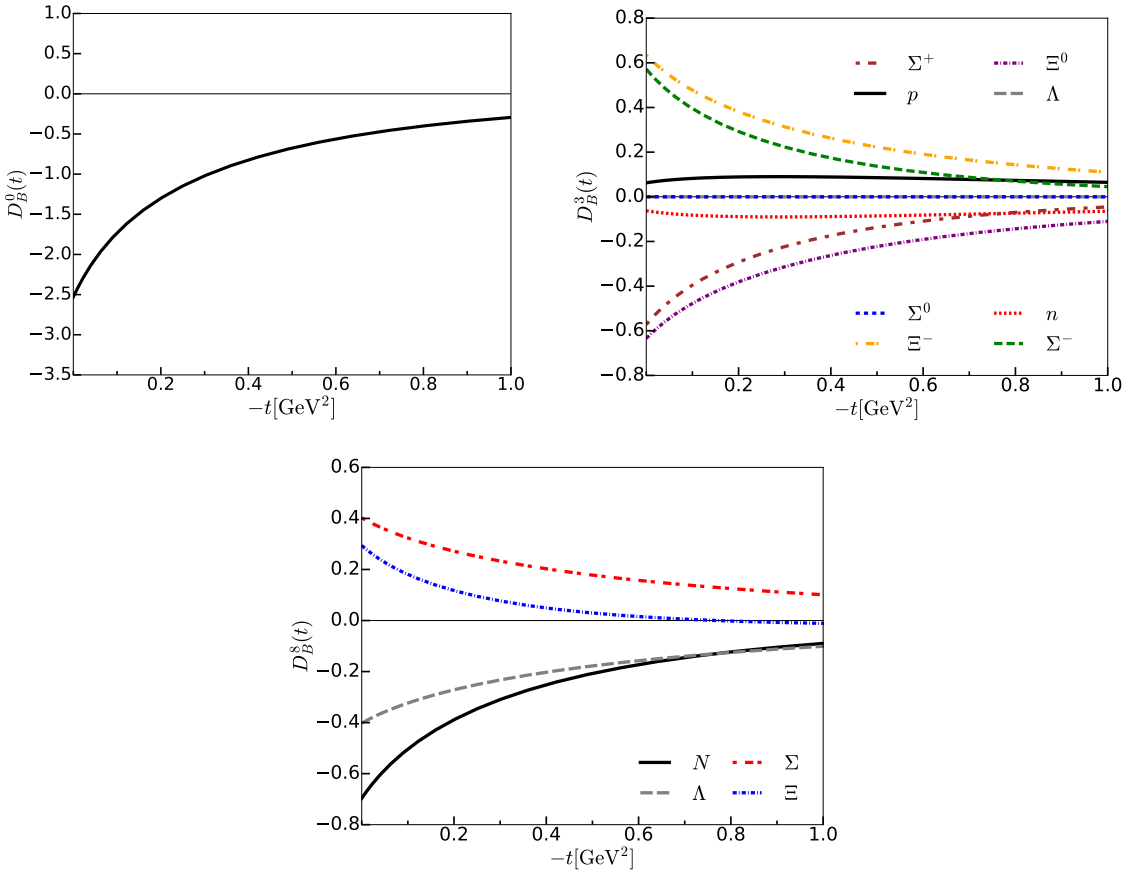

Figure 9. Flavor-singlet, -triplet, and -octet D-term form factors for the baryon octet are drawn.

pattern we have seen before. Similarly to the J^8 form factor, the flavor-octet D^8 form factors for the iso-multiplet members are degenerate, leading to the following relations:

$$\sum_{B=N,\Xi} D_B^8 \neq 0, \quad \sum_{B=\Lambda,\Sigma} D_B^8 = 0. \tag{4.27}$$

Next, we investigate the flavor-decomposed D-term form factors. Interestingly, unlike the $J(t)$ form factors for the Λ^0 and Σ^0 baryons, we find that the s-quark contributions to the D-term for the Σ^0 baryon are larger than those for the Λ^0 baryon:

$$\begin{aligned} D^u_{\Lambda^0} &= -0.960, \quad D^d_{\Lambda^0} = -0.960, \quad D^s_{\Lambda^0} = -0.611, \\ D^u_{\Sigma^0} &= -0.727, \quad D^d_{\Sigma^0} = -0.727, \quad D^s_{\Sigma^0} = -1.076. \end{aligned} \tag{4.28}$$

Similarly, for the other octet baryons p, n, Σ^+, Σ^-, Ξ^0, and Ξ^-, we find that the flavor-decomposed D^q form factors can be obtained by counting the number of valence quarks. For example, the flavor-decomposed D-term form factors for the Σ^+ baryon are given by:

$$\begin{aligned} \text{two quarks with the same flavor } (u) &\to D^u(0) = -1.014, \\ \text{one quark } (s) &\to D^s(0) = -1.076, \\ \text{non-valence quark } (d) &\to D^d(0) = -0.441. \end{aligned} \tag{4.29}$$

JHEP05(2024)173

These relations are exactly the same as the flavor-decomposed $J(t)$ form factors for the baryon octet. It is important to note that the contributions of non-valence quarks to the D-term form factors are rather significant. Therefore, these contributions should be considered in estimating the flavor-decomposed D-term form factors as they play an essential role alongside valence quarks.

Finally, we turn our attention to the generalized electromagnetic form factors (GEMFFs). The first Mellin moments of the GPDs are directly related to the EMFFs. By retaining the flavor structure of the EMFFs, we can derive the GEMFFs through the second Mellin moments of the GPDs. The flavor structure of the electromagnetic current is given by the matrix:

$$Q = \begin{pmatrix} \frac{2}{3} & 0 & 0 \\ 0 & -\frac{1}{3} & 0 \\ 1 & 0 & -\frac{1}{3} \end{pmatrix} = \frac{1}{2}\left(\lambda^3 + \frac{1}{\sqrt{3}}\lambda^8\right), \tag{4.30}$$

where λ^3 and λ^8 are Gell-Mann matrices. By inserting this flavor operator into the equation governing the electromagnetic current, eq. (3.12), we obtain the GEMFFs. These GEMFFs can be expressed as a linear combination of the flavor-triplet and -octet GFFs, namely $F_B^Q = \frac{1}{2}\left(F_B^3 + \frac{1}{\sqrt{3}}F_B^8\right)$. Similar to the EMFFs, the GEMFFs satisfy the U-spin symmetry. This symmetry implies that the GEMFFs for baryons with the same charge, except for the Λ^0 and Σ^0 baryons, are equivalent when the flavor SU(3) symmetry is imposed. In other words, we have:

$$F_p^Q(t) = F_{\Sigma^+}^Q(t), \quad F_n^Q(t) = F_{\Xi^0}^Q(t), \quad F_{\Sigma^-}^Q(t) = F_{\Xi^-}^Q(t), \quad F_{\Lambda^0}^Q(t) = -F_{\Sigma^0}^Q(t). \tag{4.31}$$

This U-spin symmetry is observed numerically in figure 10. The observed U-spin symmetry aligns with the spin-flavor relations found in the analysis of the separate flavor-singlet, -triplet, and -octet GFFs.

5 Conclusions and summary

In the current work, we focused on investigating the flavor-decomposed gravitational form factors (GFFs) for the nucleon and hyperons, and their mechanical interpretations.

Once we perform the flavor decomposition of the GFFs and distributions, the higher-twist form factor ($\bar{c}$) comes into play in the mechanical interpretation and plays an essential role. However, extracting the higher-twist form factor is challenging in the various dynamical models and lattice QCD. Therefore, we isolate this twist-4 part by performing the twist projection. We then obtain the twist-projected EMT current and define the corresponding EMT distributions.

Using the chiral quark-soliton model derived from the QCD instanton vacuum, we estimate the GFFs and the EMT distributions. Before discussing the numerical results, we have highlighted two important features:

- In the large N_c limit of QCD, the collective motion of the chiral soliton is nonrelativistic, while the internal dynamics remains fully relativistic. Therefore, we naturally adopt three-dimensional (3D) mechanical interpretations of the gravitational form factors.

JHEP05(2024)173

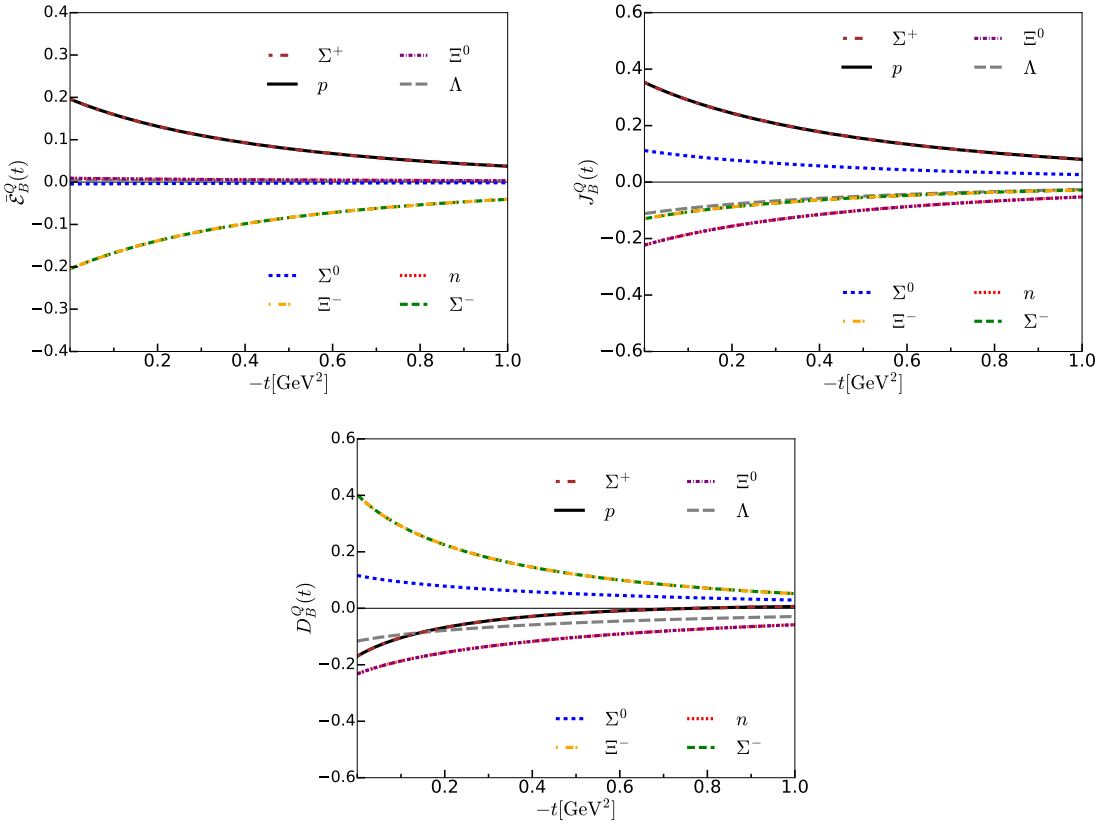

Figure 10. Generlized electromagnetic form factor for the octet baryons are drawn.

- In the effective chiral theory, the flavor-decomposed EMT current must be derived from the QCD operator which is consistent with the effective quark-gluon dynamics. In any models, such as NJL and bag models, once the effective action is given, the flavor-singlet EMT current can be derived from the global symmetry. However, there is no relevant global symmetry for the flavor triplet and octet currents. Thus, one must derive the corresponding effective operators from the QCD operator. This can be done by replacing the gluon fields by the effective quark fields through the QCD instanton vacuum.

By adopting the 3D mechanical interpretation and the twist-2 effective operator derived from the QCD instanton vacuum, we estimated the twist-2 GFFs and understood the role of the strange quark in the mechanics of the proton.

We summarize the numerical results obtained in the current work: firstly, we obtained the flavor-decomposed twist-2 mass distribution in the rest frame, which is influenced by the A. While the flavor-singlet component was properly normalized to unity, i.e., $\sum_q A_p^q(0) = 1$, no constraints were imposed on the flavor-triplet and -octet components. Our findings revealed that the light-front momentum fraction carried by up, down, and strange quarks in the proton was estimated to be 59%, 35%, and 6%.

Secondly, regarding the AM distribution, we observed that the J form factor was appropriately normalized to the proton spin, i.e, $\sum_q J^q(0) = 1/2$. We determined the fraction

JHEP05(2024)173

of the proton spin carried by up, down, and strange quarks, which were found to be $J_p^u = 0.52$, $J_p^u = -0.06$, and $J_p^s = 0.04$, respectively. Similar to the mass form factor, the strange quark contributed minimally to the proton AM. For the flavor-singlet AM, it can be decomposed into OAM and intrinsic quark spin. Each carries a half of the nucleon spin within the current framework. However, in this work, we focused on the total AM instead of the flavor-decomposed OAM due to ambiguities in matching twist-3 QCD operators with the effective operators we employed.

Thirdly, the mechanical properties of the proton were investigated. The stress tensor was parameterized in terms of the twist-2 pressure and shear-force distributions, which were obtained through three-dimensional Fourier transforms of the pressure $\mathcal{P}$ and D-term form factors. Notably, we observed that $D_p^{u-d} \sim 0$ in the flavor SU(3) sector:

$$D_p^{u-d} \sim 0.3, \quad [\mathrm{SU}(2)] \quad \text{vs.} \quad D_p^{u-d} \sim 0, \quad [\mathrm{SU}(3)]. \tag{5.1}$$

This suggests that the large N_c assumption ($D^{u-d} \sim 0$) used in extracting the D-term from the DVCS data is more appropriate for the flavor SU(3) sector, rather than for the flavor SU(2). Moreover, in the flavor SU(3), we have determined the significant strange quark contributions to the D-term form factor, i.e., $D_p^s = -0.44$.

Lastly, we explored the GFFs for hyperons. We observed the interesting spin-flavor symmetries and introduced the electromagnetic flavor structure into the GFFs, resulting in the observation of U-spin symmetries in the generalized electromagnetic form factors.

Acknowledgments

Authors want to express gratitude to Cédric Lorcé for the invaluable comments and discussions. JYK is grateful to C. Weiss and J.L. Goity for discussions on the large N_c behavior of the GFFs and the effective operator formalism. The work was supported by the Basic Science Research Program through the National Research Foundation of Korea funded by the Korean government (Ministry of Education, Science and Technology, MEST), Grant-No. 2021R1A2C2093368 and 2018R1A5A1025563 (HYW and HChK). This work was also supported by the U.S. Department of Energy, Office of Science, Office of Nuclear Physics under contract DE-AC05-06OR23177 (JYK) and by the France Excellence scholarship through Campus France funded by the French government (Ministère de l'Europe et des Affaires Étrangères), 141295X (HYW).

JHEP05(2024)173

A EMT distributions and regularization functions

We provide explicit expressions for the EMT distributions. These distributions are compiled below. We have mass distributions:

$$\begin{aligned}
\mathcal{M}(\boldsymbol{r}) &= \frac{3}{4}N_c\bigg[E_v\psi_v^\dagger(\boldsymbol{r})\psi_v(\boldsymbol{r}) + \sum_n \psi_n^\dagger(\boldsymbol{r})\psi_n(\boldsymbol{r})R_{0n}\bigg],\\
\mathcal{J}_1(\boldsymbol{r}) &= \frac{3}{16}N_c\bigg[\sum_{n\neq v}\frac{E_n+E_v}{E_n-E_v}\langle n|\tau_3|v\rangle\,\psi_v^\dagger(\boldsymbol{r})\tau_3\psi_n(\boldsymbol{r})\\
&\quad + \frac{1}{2}\sum_{n,m}(E_n+E_m)\langle n|\tau_3|m\rangle\,\psi_m^\dagger(\boldsymbol{r})\tau_3\psi_n(\boldsymbol{r})R_{3nm}\bigg],\\
\mathcal{J}_2(\boldsymbol{r}) &= \frac{3}{32}N_c\bigg[\sum_{n^0}\frac{E_{n^0}+E_v}{E_{n^0}-E_v}\Big\langle n^0\Big|v\Big\rangle\,\psi_v^\dagger(\boldsymbol{r})\psi_{n^0}(\boldsymbol{r})\\
&\quad + \sum_{n^0,m}(E_{n^0}+E_m)\Big\langle n^0\Big|m\Big\rangle\,\psi_m^\dagger(\boldsymbol{r})\psi_{n^0}(\boldsymbol{r})R_{3n^0m}\bigg],
\end{aligned}\tag{A.1}$$

and the AM distributions:

$$\begin{aligned}
\mathcal{Q}_0(\boldsymbol{r}) &= \frac{N_c}{4}\bigg[\psi_v^\dagger(\boldsymbol{r})\Gamma^J_{vv3}\tau_3\psi_v(\boldsymbol{r}) - \frac{1}{2}\sum_n \mathrm{sign}(E_n)\psi_n^\dagger(\boldsymbol{r})\Gamma^J_{nn3}\tau_3\psi_n(\boldsymbol{r})\bigg],\\
\mathcal{Q}_1(\boldsymbol{r}) &= \frac{N_c}{4}if_{ij3}\bigg[\sum_{n\neq v}\frac{\mathrm{sign}(E_n)}{E_n-E_v}\langle n|\tau_i|v\rangle\,\psi_v^\dagger(\boldsymbol{r})\tau_j\Gamma^J_{vn3}\psi_n(\boldsymbol{r})\\
&\quad + \frac{1}{2}\sum_{n,m}\langle n|\tau_i|m\rangle\,\psi_m^\dagger(\boldsymbol{r})\tau_j\Gamma^J_{mn3}\psi_n(\boldsymbol{r})R_{6nm}\bigg],\\
\mathcal{I}_1(\boldsymbol{r}) &= \frac{N_c}{4}\bigg[\sum_{n\neq v}\frac{\langle n|\tau_3|v\rangle}{E_n-E_v}\psi_v^\dagger(\boldsymbol{r})\Gamma^J_{vn3}\psi_n(\boldsymbol{r}) + \frac{1}{2}\sum_{n,m}\langle n|\tau_3|m\rangle\,\psi_m^\dagger(\boldsymbol{r})\Gamma^J_{mn3}\psi_n(\boldsymbol{r})R_{3nm}\bigg],\\
\mathcal{I}_2(\boldsymbol{r}) &= \frac{N_c}{4}\bigg[\sum_{n^0}\frac{\langle n^0|v\rangle}{E_{n^0}-E_v}\psi_v^\dagger(\boldsymbol{r})\tau_3\Gamma^J_{vn^03}\psi_{n^0}(\boldsymbol{r})\\
&\quad + \sum_{n^0,m}\Big\langle n^0\Big|m\Big\rangle\,\psi_m^\dagger(\boldsymbol{r})\tau_3\Gamma^J_{mn^03}\psi_{n^0}(\boldsymbol{r})R_{3n^0m}\bigg],
\end{aligned}\tag{A.2}$$

where $\Gamma^J_3(E_n,E_m) = \Gamma^J_{nm3} = \Big(2\hat{L}_3 + (E_n+E_m)\gamma_5(\boldsymbol{r}\times\boldsymbol{\sigma})_3\Big)$ with $\hat{\boldsymbol{L}} = \Big[\boldsymbol{r}\times\frac{i}{2}(\overleftarrow{\boldsymbol{\nabla}}-\overrightarrow{\boldsymbol{\nabla}})\Big]$. The quadrupole distributions $s(r)$ relevant for the D-term form factors are given by

$$\begin{aligned}
\mathcal{N}_1(\boldsymbol{r}) &= \frac{3}{2}N_c\left[\psi_v^\dagger(\boldsymbol{r})\Gamma^s\psi_v(\boldsymbol{r}) + \sum_n\psi_n^\dagger(\boldsymbol{r})\Gamma^s\psi_n(\boldsymbol{r})R_{1n}\right],\\
\mathcal{J}_3(\boldsymbol{r}) &= \frac{3}{4}N_c\left[\sum_{n\neq v}\frac{\langle n|\tau_3|v\rangle}{E_n-E_v}\psi_v^\dagger(\boldsymbol{r})\tau_3\Gamma^s\psi_n(\boldsymbol{r}) + \frac{1}{2}\sum_{n,m}\langle n|\tau_3|m\rangle\,\psi_m^\dagger(\boldsymbol{r})\tau_3\Gamma^s\psi_n(\boldsymbol{r})R_{5nm}\right],\\
\mathcal{J}_4(\boldsymbol{r}) &= \frac{3}{8}N_c\left[\sum_{n^0}\frac{\langle n^0|v\rangle}{E_{n^0}-E_v}\psi_v^\dagger(\boldsymbol{r})\Gamma^s\psi_{n^0}(\boldsymbol{r}) + \sum_{n^0,m}\Big\langle n^0\Big|m\Big\rangle\,\psi_m^\dagger(\boldsymbol{r})\Gamma^s\psi_{n^0}(\boldsymbol{r})R_{5n^0m}\right],
\end{aligned}\tag{A.3}$$

JHEP05(2024)173

B	Y	T	D_{38}	D_{88}	$D_{3i}J_i$	$D_{8i}J_i$	$D_{3a}J_a$	$D_{8a}J_a$
N	1	$\frac{1}{2}$	$\frac{\sqrt{3}}{15}T_3$	$\frac{3}{10}$	$-\frac{7}{10}T_3$	$-\frac{\sqrt{3}}{20}$	$-\frac{1}{5}T_3$	$-\frac{3\sqrt{3}}{10}$
Λ	0	0	0	$\frac{1}{10}$	0	$\frac{3\sqrt{3}}{20}$	0	$-\frac{\sqrt{3}}{10}$
Σ	0	1	$\frac{\sqrt{3}}{6}T_3$	$-\frac{1}{10}$	$-\frac{1}{4}T_3$	$-\frac{3\sqrt{3}}{20}$	$-\frac{1}{2}T_3$	$\frac{\sqrt{3}}{10}$
Ξ	-1	$\frac{1}{2}$	$\frac{4\sqrt{3}}{15}T_3$	$-\frac{1}{5}$	$\frac{1}{5}T_3$	$\frac{\sqrt{3}}{5}$	$-\frac{4}{5}T_3$	$\frac{\sqrt{3}}{5}$

Table 2. The matrix elements of the spin-flavor operators relevant to T^{00} and T^{ij} are listed.

where $\Gamma^s = \gamma^0\left(\hat{\boldsymbol{n}}\cdot\boldsymbol{p}\right) - \frac{1}{3}\gamma^0\left(\boldsymbol{\gamma}\cdot\boldsymbol{p}\right)$). The moments of inertia I_1 and I_2 are written as follows:

$$
\begin{aligned}
I_1 &= \frac{N_c}{2}\left[\sum_{n\neq v}\frac{1}{E_n - E_v}\langle n|\tau_3|v\rangle\ \langle v|\tau_3|n\rangle + \frac{1}{2}\sum_{n,m}\langle n|\tau_3|m\rangle\ \langle m|\tau_3|n\rangle\, R_{3nm}\right],\\
I_2 &= \frac{N_c}{4}\left[\sum_{n^0}\frac{1}{E_{n^0} - E_v}\left\langle n^0\middle|v\right\rangle\left\langle v\middle|n^0\right\rangle + \sum_{n^0,m}\left\langle n^0\middle|m\right\rangle\left\langle m\middle|n^0\right\rangle R_{3n^0m}\right].
\end{aligned}
\tag{A.4}
$$

In addition, all distributions are regularized, and their regularization functions are written as

$$
\begin{aligned}
R_0(E_n) := R_{0n} &= \frac{1}{4\sqrt{\pi}}\int_{\Lambda^{-2}}\frac{du}{u^{3/2}}e^{-uE_n^2},\\
R_1(E_n) := R_{1n} &= -\frac{E_n}{2\sqrt{\pi}}\int_{\Lambda^{-2}}\frac{du}{\sqrt{u}}e^{-uE_n^2},\\
R_3(E_n,E_m) := R_{3nm} &= \frac{1}{2\sqrt{\pi}}\int_{\Lambda^{-2}}\frac{du}{\sqrt{u}}\left[\frac{1}{u}\frac{e^{-uE_n^2} - e^{-uE_m^2}}{E_m^2 - E_n^2} - \frac{E_n e^{-uE_n^2} + E_m e^{-uE_m^2}}{E_n + E_m}\right],\\
R_5(E_n,E_m) := R_{5nm} &= \frac{1}{2}\frac{\mathrm{sign}(E_n) - \mathrm{sign}(E_m)}{E_n - E_m},\\
R_6(E_n,E_m) := R_{6nm} &= \frac{1 - \mathrm{sign}(E_n)\mathrm{sign}(E_m)}{E_n - E_m},
\end{aligned}
\tag{A.5}
$$

with $\psi_v(\boldsymbol{r}) := \langle\boldsymbol{r}|v\rangle$ and $\psi_n(\boldsymbol{r}) := \langle\boldsymbol{r}|n\rangle$.

B Matrix elements of the spin-flavor operators

In appendix B we list the matrix elements of the spin-flavor operators relevant to T^{00} and T^{ij} in table 2, and those relevant to T^{0k} in table 3.

JHEP05(2024)173

B	Y	T	D_{33}	D_{83}	$D_{38}J_3$	$D_{88}J_3$	$d_{ab3}D_{3a}J_b$	$d_{ab3}D_{8a}J_b$
N	1	$\frac{1}{2}$	$-\frac{14}{15}T_3J_3$	$-\frac{\sqrt{3}}{15}J_3$	$\frac{\sqrt{3}}{15}T_3J_3$	$\frac{3}{10}J_3$	$\frac{7}{15}T_3J_3$	$\frac{\sqrt{3}}{30}J_3$
Λ	0	0	0	$\frac{\sqrt{3}}{5}J_3$	0	$\frac{1}{10}J_3$	0	$-\frac{\sqrt{3}}{10}J_3$
Σ	0	1	$-\frac{1}{3}T_3J_3$	$-\frac{\sqrt{3}}{5}J_3$	$\frac{\sqrt{3}}{6}T_3J_3$	$-\frac{1}{10}J_3$	$\frac{1}{6}T_3J_3$	$\frac{\sqrt{3}}{10}J_3$
Ξ	-1	$\frac{1}{2}$	$\frac{4}{15}T_3J_3$	$\frac{4\sqrt{3}}{15}J_3$	$\frac{4\sqrt{3}}{15}T_3J_3$	$-\frac{1}{5}J_3$	$-\frac{2}{15}T_3J_3$	$-\frac{2\sqrt{3}}{15}J_3$

Table 3. The matrix elements of the spin-flavor operators relevant to T^{0k} are listed.

References

[1] European Muon collaboration, *A Measurement of the Spin Asymmetry and Determination of the Structure Function g(1) in Deep Inelastic Muon-Proton Scattering*, *Phys. Lett. B* **206** (1988) 364 [INSPIRE].

[2] European Muon collaboration, *An Investigation of the Spin Structure of the Proton in Deep Inelastic Scattering of Polarized Muons on Polarized Protons*, *Nucl. Phys. B* **328** (1989) 1 [INSPIRE].

[3] C.A. Aidala, S.D. Bass, D. Hasch and G.K. Mallot, *The Spin Structure of the Nucleon*, *Rev. Mod. Phys.* **85** (2013) 655 [arXiv:1209.2803] [INSPIRE].

[4] D.B. Kaplan and A. Manohar, *Strange Matrix Elements in the Proton from Neutral Current Experiments*, *Nucl. Phys. B* **310** (1988) 527 [INSPIRE].

[5] E.J. Beise, M.L. Pitt and D.T. Spayde, *The SAMPLE experiment and weak nucleon structure*, *Prog. Part. Nucl. Phys.* **54** (2005) 289 [nucl-ex/0412054] [INSPIRE].

[6] A4 collaboration, *Measurement of strange quark contributions to the nucleon's form-factors at* $Q^2 = 0.230\,(GeV/c)^2$, *Phys. Rev. Lett.* **93** (2004) 022002 [nucl-ex/0401019] [INSPIRE].

[7] F.E. Maas et al., *Evidence for strange quark contributions to the nucleon's form-factors at* $q^2 = 0.108\,(GeV/c)^2$, *Phys. Rev. Lett.* **94** (2005) 152001 [nucl-ex/0412030] [INSPIRE].

[8] HAPPEX collaboration, *Parity-violating electron scattering from He-4 and the strange electric form-factor of the nucleon*, *Phys. Rev. Lett.* **96** (2006) 022003 [nucl-ex/0506010] [INSPIRE].

[9] G0 collaboration, *Strange quark contributions to parity-violating asymmetries in the forward G0 electron-proton scattering experiment*, *Phys. Rev. Lett.* **95** (2005) 092001 [nucl-ex/0506021] [INSPIRE].

[10] G0 collaboration, *Strange Quark Contributions to Parity-Violating Asymmetries in the Backward Angle G0 Electron Scattering Experiment*, *Phys. Rev. Lett.* **104** (2010) 012001 [arXiv:0909.5107] [INSPIRE].

[11] F.E. Maas and K.D. Paschke, *Strange nucleon form-factors*, *Prog. Part. Nucl. Phys.* **95** (2017) 209 [INSPIRE].

[12] B. Borasoy and U.-G. Meissner, *Chiral Expansion of Baryon Masses and* σ*-Terms*, *Annals Phys.* **254** (1997) 192 [hep-ph/9607432] [INSPIRE].

[13] H.-C. Kim, M.V. Polyakov and K. Goeke, *Tensor charges of the nucleon in the SU(3) chiral quark soliton model*, *Phys. Lett. B* **387** (1996) 577 [hep-ph/9604442] [INSPIRE].

JHEP05(2024)173

[14] T. Ledwig, A. Silva and H.-C. Kim, *Tensor charges and form factors of SU(3) baryons in the self-consistent SU(3) chiral quark-soliton model*, *Phys. Rev. D* **82** (2010) 034022 [arXiv:1004.3612] [INSPIRE].

[15] I.Y. Kobzarev and L.B. Okun, *Gravitational interaction of fermions*, *Zh. Eksp. Teor. Fiz.* **43** (1962) 1904 [INSPIRE].

[16] H. Pagels, *Energy-Momentum Structure Form Factors of Particles*, *Phys. Rev.* **144** (1966) 1250 [INSPIRE].

[17] X.-D. Ji, *Gauge-Invariant Decomposition of Nucleon Spin*, *Phys. Rev. Lett.* **78** (1997) 610 [hep-ph/9603249] [INSPIRE].

[18] M.V. Polyakov, *Generalized parton distributions and strong forces inside nucleons and nuclei*, *Phys. Lett. B* **555** (2003) 57 [hep-ph/0210165] [INSPIRE].

[19] D. Müller et al., *Wave functions, evolution equations and evolution kernels from light ray operators of QCD*, *Fortsch. Phys.* **42** (1994) 101 [hep-ph/9812448] [INSPIRE].

[20] X.-D. Ji, *Deeply virtual Compton scattering*, *Phys. Rev. D* **55** (1997) 7114 [hep-ph/9609381] [INSPIRE].

[21] A.V. Radyushkin, *Scaling limit of deeply virtual Compton scattering*, *Phys. Lett. B* **380** (1996) 417 [hep-ph/9604317] [INSPIRE].

[22] A.V. Radyushkin, *Asymmetric gluon distributions and hard diffractive electroproduction*, *Phys. Lett. B* **385** (1996) 333 [hep-ph/9605431] [INSPIRE].

[23] X.-D. Ji, *Breakup of hadron masses and energy - momentum tensor of QCD*, *Phys. Rev. D* **52** (1995) 271 [hep-ph/9502213] [INSPIRE].

[24] M.V. Polyakov and P. Schweitzer, *Forces inside hadrons: pressure, surface tension, mechanical radius, and all that*, *Int. J. Mod. Phys. A* **33** (2018) 1830025 [arXiv:1805.06596] [INSPIRE].

[25] J. Balla, M.V. Polyakov and C. Weiss, *Nucleon matrix elements of higher twist operators from the instanton vacuum*, *Nucl. Phys. B* **510** (1998) 327 [hep-ph/9707515] [INSPIRE].

[26] D. Diakonov, M.V. Polyakov and C. Weiss, *Hadronic matrix elements of gluon operators in the instanton vacuum*, *Nucl. Phys. B* **461** (1996) 539 [hep-ph/9510232] [INSPIRE].

[27] E. Witten, *Baryons in the 1/n Expansion*, *Nucl. Phys. B* **160** (1979) 57 [INSPIRE].

[28] E. Witten, *Current Algebra, Baryons, and Quark Confinement*, *Nucl. Phys. B* **223** (1983) 433 [INSPIRE].

[29] R.F. Dashen and A.V. Manohar, *Baryon - pion couplings from large N(c) QCD*, *Phys. Lett. B* **315** (1993) 425 [hep-ph/9307241] [INSPIRE].

[30] R.F. Dashen, E.E. Jenkins and A.V. Manohar, *The 1/N(c) expansion for baryons*, *Phys. Rev. D* **49** (1994) 4713 [*Erratum ibid.* **51** (1995) 2489] [hep-ph/9310379] [INSPIRE].

[31] R.F. Dashen, E.E. Jenkins and A.V. Manohar, *Spin flavor structure of large N(c) baryons*, *Phys. Rev. D* **51** (1995) 3697 [hep-ph/9411234] [INSPIRE].

[32] D. Diakonov and V.Y. Petrov, *A Theory of Light Quarks in the Instanton Vacuum*, *Nucl. Phys. B* **272** (1986) 457 [INSPIRE].

[33] D. Diakonov, *Instantons at work*, *Prog. Part. Nucl. Phys.* **51** (2003) 173 [hep-ph/0212026] [INSPIRE].

[34] A. Blotz, M. Praszalowicz and K. Goeke, *Gottfried sum in the SU(3) NJL model*, *Phys. Rev. D* **53** (1996) 551 [INSPIRE].

JHEP05(2024)173

[35] P.V. Pobylitsa et al., *Isovector unpolarized quark distribution in the nucleon in the large N(c) limit*, *Phys. Rev. D* **59** (1999) 034024 [hep-ph/9804436] [INSPIRE].

[36] D. Diakonov et al., *Nucleon parton distributions at low normalization point in the large N(c) limit*, *Nucl. Phys. B* **480** (1996) 341 [hep-ph/9606314] [INSPIRE].

[37] D. Diakonov et al., *Unpolarized and polarized quark distributions in the large N(c) limit*, *Phys. Rev. D* **56** (1997) 4069 [hep-ph/9703420] [INSPIRE].

[38] M. Wakamatsu and T. Kubota, *Chiral symmetry and the nucleon spin structure functions*, *Phys. Rev. D* **60** (1999) 034020 [hep-ph/9809443] [INSPIRE].

[39] H.-C. Kim, M.V. Polyakov and K. Goeke, *Nucleon tensor charges in the SU(2) chiral quark - soliton model*, *Phys. Rev. D* **53** (1996) 4715 [hep-ph/9509283] [INSPIRE].

[40] P. Schweitzer et al., *Transversity distributions in the nucleon in the large N(c) limit*, *Phys. Rev. D* **64** (2001) 034013 [hep-ph/0101300] [INSPIRE].

[41] M. Wakamatsu, *Chiral odd distribution functions in the chiral quark soliton model*, *Phys. Lett. B* **509** (2001) 59 [hep-ph/0012331] [INSPIRE].

[42] A. Blotz, M.V. Polyakov and K. Goeke, *The spin of the proton in the solitonic SU(3) NJL model*, *Phys. Lett. B* **302** (1993) 151 [INSPIRE].

[43] A. Blotz, M. Praszalowicz and K. Goeke, *Axial properties of the nucleon with 1/N(c) corrections in the solitonic SU(3) NJL model*, *Phys. Rev. D* **53** (1996) 485 [hep-ph/9403314] [INSPIRE].

[44] H.-C. Kim, A. Blotz, C. Schneider and K. Goeke, *Strangeness in the scalar form-factor of the nucleon*, *Nucl. Phys. A* **596** (1996) 415 [hep-ph/9508299] [INSPIRE].

[45] A. Silva, H.-C. Kim and K. Goeke, *Strange form-factors in the context of SAMPLE, HAPPEX, and A4 experiments*, *Phys. Rev. D* **65** (2002) 014016 [*Erratum ibid.* **66** (2002) 039902] [hep-ph/0107185] [INSPIRE].

[46] C.V. Christov et al., *Baryons as nontopological chiral solitons*, *Prog. Part. Nucl. Phys.* **37** (1996) 91 [hep-ph/9604441] [INSPIRE].

[47] M. Wakamatsu and H. Yoshiki, *A chiral quark model of the nucleon*, *Nucl. Phys. A* **524** (1991) 561 [INSPIRE].

[48] K. Goeke et al., *Nucleon form-factors of the energy momentum tensor in the chiral quark-soliton model*, *Phys. Rev. D* **75** (2007) 094021 [hep-ph/0702030] [INSPIRE].

[49] D.R. Yennie, M.M. Lévy and D.G. Ravenhall, *Electromagnetic Structure of Nucleons*, *Rev. Mod. Phys.* **29** (1957) 144 [INSPIRE].

[50] M. Burkardt, *Impact parameter dependent parton distributions and off forward parton distributions for $\zeta \to 0$*, *Phys. Rev. D* **62** (2000) 071503 [*Erratum ibid.* **66** (2002) 119903] [hep-ph/0005108] [INSPIRE].

[51] M. Burkardt, *Impact parameter space interpretation for generalized parton distributions*, *Int. J. Mod. Phys. A* **18** (2003) 173 [hep-ph/0207047] [INSPIRE].

[52] G.A. Miller, *Charge Density of the Neutron*, *Phys. Rev. Lett.* **99** (2007) 112001 [arXiv:0705.2409] [INSPIRE].

[53] R.L. Jaffe, *Ambiguities in the definition of local spatial densities in light hadrons*, *Phys. Rev. D* **103** (2021) 016017 [arXiv:2010.15887] [INSPIRE].

[54] A.V. Belitsky and A.V. Radyushkin, *Unraveling hadron structure with generalized parton distributions*, *Phys. Rept.* **418** (2005) 1 [hep-ph/0504030] [INSPIRE].

JHEP05(2024)173

[55] C. Lorcé, P. Schweitzer and K. Tezgin, *2D energy-momentum tensor distributions of nucleon in a large-Nc quark model from ultrarelativistic to nonrelativistic limit*, *Phys. Rev. D* **106** (2022) 014012 [arXiv:2202.01192] [INSPIRE].

[56] J.-Y. Kim, H.-Y. Won, J.L. Goity and C. Weiss, *QCD angular momentum in $N \to \Delta$ transitions*, *Phys. Lett. B* **844** (2023) 138083 [arXiv:2304.08575] [INSPIRE].

[57] Y. Chen and C. Lorcé, *Pion and nucleon relativistic electromagnetic four-current distributions*, *Phys. Rev. D* **106** (2022) 116024 [arXiv:2210.02908] [INSPIRE].

[58] E. Leader and C. Lorcé, *The angular momentum controversy: What's it all about and does it matter?*, *Phys. Rept.* **541** (2014) 163 [arXiv:1309.4235] [INSPIRE].

[59] C. Lorcé, L. Mantovani and B. Pasquini, *Spatial distribution of angular momentum inside the nucleon*, *Phys. Lett. B* **776** (2018) 38 [arXiv:1704.08557] [INSPIRE].

[60] I.Y. Kobsarev and V.I. Zakharov, *Consequences of the transversality of the graviton emission amplitude*, *Annals Phys.* **60** (1970) 448 [INSPIRE].

[61] K.L. Ng, *Gravitational form-factors of the neutrino*, *Phys. Rev. D* **47** (1993) 5187 [gr-qc/9305002] [INSPIRE].

[62] S. Cotogno, C. Lorcé, P. Lowdon and M. Morales, *Covariant multipole expansion of local currents for massive states of any spin*, *Phys. Rev. D* **101** (2020) 056016 [arXiv:1912.08749] [INSPIRE].

[63] J.-Y. Kim, *Parametrization of transition energy-momentum tensor form factors*, *Phys. Lett. B* **834** (2022) 137442 [arXiv:2206.10202] [INSPIRE].

[64] G.A. Miller, *Transverse Charge Densities*, *Ann. Rev. Nucl. Part. Sci.* **60** (2010) 1 [arXiv:1002.0355] [INSPIRE].

[65] R.G. Sachs, *High-Energy Behavior of Nucleon Electromagnetic Form Factors*, *Phys. Rev.* **126** (1962) 2256 [INSPIRE].

[66] C. Lorcé, *Charge Distributions of Moving Nucleons*, *Phys. Rev. Lett.* **125** (2020) 232002 [arXiv:2007.05318] [INSPIRE].

[67] Y. Chen and C. Lorcé, *Nucleon relativistic polarization and magnetization distributions*, *Phys. Rev. D* **107** (2023) 096003 [arXiv:2302.04672] [INSPIRE].

[68] C. Lorcé and P. Wang, *Deuteron relativistic charge distributions*, *Phys. Rev. D* **105** (2022) 096032 [arXiv:2204.01465] [INSPIRE].

[69] E. Epelbaum et al., *Definition of Local Spatial Densities in Hadrons*, *Phys. Rev. Lett.* **129** (2022) 012001 [arXiv:2201.02565] [INSPIRE].

[70] J.Y. Panteleeva, E. Epelbaum, J. Gegelia and U.-G. Meißner, *Definition of electromagnetic local spatial densities for composite spin-1/2 systems*, *Phys. Rev. D* **106** (2022) 056019 [arXiv:2205.15061] [INSPIRE].

[71] H. Alharazin et al., *Local spatial densities for composite spin-3/2 systems*, *JHEP* **02** (2023) 163 [arXiv:2212.11505] [INSPIRE].

[72] P. Schweitzer and K. Tezgin, *Monopole and quadrupole contributions to the angular momentum density*, *Phys. Lett. B* **796** (2019) 47 [arXiv:1905.12336] [INSPIRE].

[73] J.-Y. Kim and C. Weiss, *Instanton effects in twist-3 generalized parton distributions*, *Phys. Lett. B* **848** (2024) 138387 [arXiv:2310.16890] [INSPIRE].

JHEP05(2024)173

[74] J.-Y. Kim, H.-Y. Won, H.-C. Kim and C. Weiss, *Spin-orbit correlations in the nucleon in the large-N_c limit*, arXiv:2403.07186 [INSPIRE].

[75] I.A. Perevalova, M.V. Polyakov and P. Schweitzer, *On LHCb pentaquarks as a baryon-$\psi(2S)$ bound state: prediction of isospin-$\frac{3}{2}$ pentaquarks with hidden charm*, *Phys. Rev. D* **94** (2016) 054024 [arXiv:1607.07008] [INSPIRE].

[76] M.V. Polyakov and P. Schweitzer, *Mechanical properties of particles*, *PoS* **SPIN2018** (2019) 066 [arXiv:1812.06143] [INSPIRE].

[77] C. Lorcé, H. Moutarde and A.P. Trawiński, *Revisiting the mechanical properties of the nucleon*, *Eur. Phys. J. C* **79** (2019) 89 [arXiv:1810.09837] [INSPIRE].

[78] K. Goeke, J. Ossmann, P. Schweitzer and A. Silva, *Pion mass dependence of the nucleon mass and chiral extrapolation of lattice data in the chiral quark soliton model*, *Eur. Phys. J. A* **27** (2006) 77 [hep-lat/0505010] [INSPIRE].

[79] M.J. Neubelt et al., *Energy momentum tensor and the D-term in the bag model*, *Phys. Rev. D* **101** (2020) 034013 [arXiv:1911.08906] [INSPIRE].

[80] H.-Y. Won, H.-C. Kim and J.-Y. Kim, *Flavor structure of the energy-momentum tensor form factors of the proton*, *Phys. Lett. B* **850** (2024) 138489 [arXiv:2302.02974] [INSPIRE].

[81] H.-Y. Won, H.-C. Kim and J.-Y. Kim, *Role of strange quarks in the D-term and cosmological constant term of the proton*, *Phys. Rev. D* **108** (2023) 094018 [arXiv:2307.00740] [INSPIRE].

[82] M. Wakamatsu and H. Tsujimoto, *The generalized parton distribution functions and the nucleon spin sum rules in the chiral quark soliton model*, *Phys. Rev. D* **71** (2005) 074001 [hep-ph/0502030] [INSPIRE].

[83] M. Wakamatsu and Y. Nakakoji, *Generalized form factors, generalized parton distributions and the spin contents of the nucleon*, *Phys. Rev. D* **74** (2006) 054006 [hep-ph/0605279] [INSPIRE].

[84] M. Wakamatsu, *On the D-term of the nucleon generalized parton distributions*, *Phys. Lett. B* **648** (2007) 181 [hep-ph/0701057] [INSPIRE].

[85] J.-Y. Kim and C. Weiss, in preparation.

[86] B.L. Ioffe, *Calculation of Baryon Masses in Quantum Chromodynamics*, *Nucl. Phys. B* **188** (1981) 317 [INSPIRE].

[87] H.-Y. Won, J.-Y. Kim and H.-C. Kim, *Gravitational form factors of the baryon octet with flavor SU(3) symmetry breaking*, *Phys. Rev. D* **106** (2022) 114009 [arXiv:2210.03320] [INSPIRE].

[88] M.V. Polyakov and H.-D. Son, *Nucleon gravitational form factors from instantons: forces between quark and gluon subsystems*, *JHEP* **09** (2018) 156 [arXiv:1808.00155] [INSPIRE].

[89] LHPC collaboration, *Nucleon structure from mixed action calculations using 2+1 flavors of asqtad sea and domain wall valence fermions*, *Phys. Rev. D* **82** (2010) 094502 [arXiv:1001.3620] [INSPIRE].

[90] K. Goeke et al., *The pion mass dependence of the nucleon form-factors of the energy momentum tensor in the chiral quark-soliton model*, *Phys. Rev. C* **75** (2007) 055207 [hep-ph/0702031] [INSPIRE].

[91] M. Wakamatsu and Y. Nakakoji, *Phenomenological analysis of the nucleon spin contents and their scale dependence*, *Phys. Rev. D* **77** (2008) 074011 [arXiv:0712.2079] [INSPIRE].

[92] J.-Y. Kim, H.-C. Kim, M.V. Polyakov and H.-D. Son, *Strong force fields and stabilities of the nucleon and singly heavy baryon Σ_c*, *Phys. Rev. D* **103** (2021) 014015 [arXiv:2008.06652] [INSPIRE].

JHEP05(2024)173

[93] J. Ossmann et al., *The generalized parton distribution function $(E^u + E^d)(x, \xi, t)$ of the nucleon in the chiral quark soliton model*, *Phys. Rev. D* **71** (2005) 034011 [hep-ph/0411172] [INSPIRE].

[94] J.-Y. Kim, *Quark distribution functions and spin-flavor structures in $N \to \Delta$ transitions*, *Phys. Rev. D* **108** (2023) 034024 [arXiv:2305.12714] [INSPIRE].

[95] V.D. Burkert, L. Elouadrhiri and F.X. Girod, *The pressure distribution inside the proton*, *Nature* **557** (2018) 396 [INSPIRE].

[96] QCDSF collaboration, *Generalized parton distributions from lattice QCD*, *Phys. Rev. Lett.* **92** (2004) 042002 [hep-ph/0304249] [INSPIRE].

[97] LHPC collaboration, *Nucleon Generalized Parton Distributions from Full Lattice QCD*, *Phys. Rev. D* **77** (2008) 094502 [arXiv:0705.4295] [INSPIRE].

[98] D.C. Hackett, D.A. Pefkou and P.E. Shanahan, *Gravitational form factors of the proton from lattice QCD*, arXiv:2310.08484 [INSPIRE].

[99] J.-M. Suh, J.-Y. Kim, G.-S. Yang and H.-C. Kim, *Quark spin content of SU(3) light and singly heavy baryons*, *Phys. Rev. D* **106** (2022) 054032 [arXiv:2208.04447] [INSPIRE].

JHEP05(2024)173